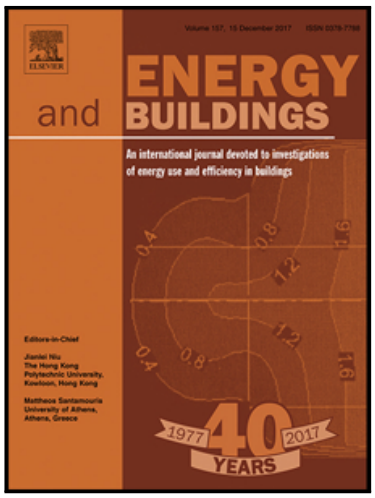

Optimization of phase change materials (PCMs) to improve energy performance within thermal comfort range in the South Korean climate

Ji Hun Park , Jongki Lee , Seunghwan Wi , Ji Soo Jeon , Seong Jin Chang , Sumin Kim

PII: S0378-7788(18)32854-8
DOI: https://doi.org/10.1016/j.enbuild.2018.12.013
Reference: ENB 8942

To appear in: *Energy & Buildings*

Received date: 12 September 2018
Revised date: 29 October 2018
Accepted date: 13 December 2018

Please cite this article as: Ji Hun Park , Jongki Lee , Seunghwan Wi , Ji Soo Jeon , Seong Jin Chang , Sumin Kim , Optimization of phase change materials (PCMs) to improve energy performance within thermal comfort range in the South Korean climate, *Energy & Buildings* (2018), doi: https://doi.org/10.1016/j.enbuild.2018.12.013

Highlights

- Optimization of PCM within comfort temperature in South Korean climate was investigated.
- PCM melting temperature of 24 ℃ were optimized in cooling.
- PCM melting temperature of 21 ℃ were optimized in heating.
- There are many variables to improve the efficiency of PCM for energy saving.

Optimization of phase change materials (PCMs) to improve energy performance within thermal comfort range in the South Korean climate

Ji Hun Park[1], Jongki Lee[2], Seunghwan Wi[1], Ji Soo Jeon[1], Seong Jin Chang[2], and Sumin Kim[1*]

[a]Building Environment & Materials Lab, Department of Architecture & Architectural Engineering, Yonsei University, Seoul 03722, Republic of Korea

[b]School of Architecture, Soongsil University, Seoul 06978, Republic of Korea

[*]Corresponding author: E-mail: kimsumin@yonsei.ac.kr

Abstract

Worldwide growth and the pursuit of comfort in buildings have led to significant increase in energy consumption, which is considered a current issue. Phase change material (PCM), a thermal energy storage (TES) material, is considered an effective and promising material to reduce energy

consumption. In recent years, research on the application of PCM to provide higher comfort for occupants has been growing rapidly. Studies show that it is necessary to consider the optimized phase change temperature of PCMs within the comfort temperature and specific climate conditions. Thus, the objective of this study is to investigate the best optimized PCM under thermal comfort range in the climate conditions of South Korea, and analyze the energy savings of PCMs, using DesignBuilder. The prepared PCMs were *n*-octadecane (OT), *n*-heptadecane (HT), and *n*-hexadecane (HX), which phase change temperatures were close to the thermal comfort range. The results of the circulation water bath test showed that the phase change temperature of the mixed PCMs by OT and HT was (22–23) °C, within the thermal comfort range. According to the various mixing ratios of OT to HT, the phase change temperatures of PCMs for OH91, OH73, OH55, OH37, and OH19 appeared at ((24–26), (23–24), (22–23), (21–23), and (20-22)) ℃, respectively. For energy simulation, gypsum boards with OT, OHs, and HT were prepared, and analyzed by replacing conventional gypsum board of the standard residential construction house model in South Korea. As a result, the maximum energy savings were shown by OH73 in cooling, and OH19 in heating. Consequently, the maximum total energy savings were achieved for OH73, which means that the best optimized PCM for South Korea demonstrated a phase change temperature of (23–24) ℃.

Keywords

Optimization; Phase change material; Thermal energy storage; Energy performance; Building energy simulation; Thermal comfort;

1. Introduction

The significant increase in energy consumption due to population growth and rapid economic growth worldwide over the past few decades is considered a current issue, especially in the building sector [1]. Furthermore, the pursuit of comfort in buildings has led to accelerating building energy consumption [2].

Thus, it is necessary to reduce the environmental load by improving energy efficiency and reducing energy consumption in the building sector. In recent years, many studies on the Thermal Energy Storage (TES) system, one of the most efficient technologies for saving energy resources, have been actively performed for the reduction of energy consumption [3]. TES systems provide superior system performance, energy efficiency, low CO_2 emissions, etc. [4], and are classified into thermochemical [5], sensible [6], and latent heat energy storage.

As one of the preferred TES methods, Phase change materials (PCMs) are thermal storage materials that use latent heat energy storage (LHES), which is considered to be the most effective and most promising system to store and discharge thermal energy [7]. The LHES of PCM depends on the phase change process storing and releasing thermal energy at a constant temperature [8, 9].

Basically, types of PCM are classified into two main categories; organic PCM and inorganic PCM [10]. Organic PCMs involving paraffin and non-paraffin [11] have the characteristics of chemical stabilization, non-toxicity, and large temperature range, but are flammable, and provide low thermal conductivity [12]. Inorganic PCMs are classified into salt hydrates and metallic, and demonstrate good thermal conductivity and high latent heat capacity; however, they are not non-flammable. They have other drawbacks, which include super-cooling and decomposition [13–16]. In addition, the liquid phase change of PCM has difficulty in application due to the phase instability, so that the PCM requires shape stabilization. To address this problem, many researchers have studied the procedures that can prevent the leaking of liquid PCM using shape-stabilized PCM (SSPCM) [17–24], microencapsulated PCM (MPCM) [25–29], macro-packed PCM (MPPCM) [30–32], and the direct incorporation of PCM techniques [33–35].

In recent years, research on the application of PCM to provide higher comfort for occupants has been growing rapidly [36–42]. As an example, Jamil et al. [43] analyzed the potential of PCM improving occupant thermal comfort in the natural-ventilated house located in Melbourne, Australia. The study investigated the most efficient PCM having suitable phase change temperature for the Melbourne climate; PCM with melting point of 25 ℃ proved to be the best PCM, and showed 34 % reduction of energy consumption. In addition, Chang et al. [44] investigated the correlation between

the indoor temperature and phase change temperature of PCM. They showed the thermal performance of n-octadecane under the heating and non-heating condition of the laboratory. The PCM maintained 28 ℃ during the non-heating time, since the temperature of the laboratory was similar to the melting point of n-octadecane. Furthermore, n-octadecane showed the best thermal performance among the specimen of PCMs. Thus, optimized application of PCMs for occupant comfort is dependent on the indoor temperature and the climate conditions of specific areas.

The objective of this study is to investigate the best optimized PCM for indoor temperature with thermal comfort range in the climate conditions of South Korea, and analyze the energy savings of PCMs. According to ISO 13790, the average thermal comfort ranges in residential building are (20 to 26) ℃ [45]. PCMs with optimized phase change temperature were prepared by mixing paraffinic PCMs that are close to the thermal comfort range: *n*-octadecane, *n*-heptadecane, and *n*-hexadecane. In order to investigate the phase change temperature of pure PCMs and mixed PCMs, the circulation water bath test was performed. Differential scanning calorimetry (DSC: Q 1000), Fourier transform infrared spectrometry (FTIR), and thermal conductivity analysis were performed to analyze the properties and chemical stability of the PCMs. In addition, the energy savings of the PCMs were analyzed by energy simulation program.

2. Experimental

2.1. *Materials*

The PCMs *n*-octadecane ($C_{18}H_{38}$), *n*-heptadecane ($C_{17}H_{36}$), and *n*-hexadecane ($C_{16}H_{34}$) are made of the alkane series, and are organic PCMs. Table 1 shows the physical properties of *n*-octadecane, *n*-heptadecane, and *n*-hexadecane. These were obtained from the Celsius Korea Corporation, South Korea, and the Sigma-Aldrich Corporation [1, 46]. The phase change temperature of these PCMs are (28.0, 22.0, and 18.0) ℃, close to the comfort temperature, which is (20–26) ℃. Thus, these were selected as TES materials, suitable for building applications.

2.2. *Optimized PCMs preparation*

To investigate the optimized PCM under the thermal comfort range, the circulation water bath test was performed, and Table 2 shows the test specimens. The pure PCMs are *n*-octadecane (OT), *n*-heptadecane (HT), and *n*-hexadecane (HX). Mixed PCMs were prepared by mixing OT, HT, and HX under 1:1 ratio, respectively, and named OTHT, OTHX, and HTHX. Figure 1 shows the procedure of the circulation water bath test. Such test procedure has been described in previous study [47]. The six prepared PCMs were placed in glass bottles, respectively, and the glass bottles with PCMs were fixed to the holder. In addition, they were immersed in water in a circulation bath (WCB-22 by DAIHAN Scientific Co., Ltd.). For the temperature conditions of the bath, the heating was set from (15 to 30) ℃, increasing by 5 ℃ per hour, and the cooling was set from (30 to 15) ℃, decreasing by 10 ℃ per hour. The cooling rate was different from the heating rate in order to clarify the

temperature change, since the cooling took longer to change the temperature than the heating. Temperature sensors were inserted in each glass bottle to measure the temperature changes by using a data logger (Logger GL820 by Graphtec).

2.3. *Characterization techniques*

The thermal properties of the PCMs, such as the melting and freezing temperatures and the latent heat capacities, were measured by using DSC. The melting and freezing temperatures were measured by drawing a line at the point of the maximum slope of the leading edge of the peak, and extrapolating to the base line. DSC measurements were performed at a 5 ℃/min heating and cooling rate over temperature ranges from (0 to 80) ℃ using Advanced T-Zero Technology [48]. The latent heat capacities of the PCM were determined by numerical integration of the area under the peaks that represent the solid–solid and solid–liquid phase transitions [49]. The error of the DSC scan rate is less than 5 %, so that the measurement condition of 5 ℃/min is considered appropriate [50].

The enthalpy values of PCMs were obtained from universal analysis and C_p-calculation programs, which converted the heat flow of DSC data to a specific heat value. The final enthalpy value was obtained from the sum of specific heat values up to 80 ℃. The thermal conductivities of specimens were measured by TCi thermal conductivity analyzer (C-Therm Technologies Ltd). TCi analyzer measures the thermal conductivity of the specimens by using the Modified Transient Plane Source

(MTPS) method [51]. The FTIR analysis (Nicolet 6700) was measured in the range (650–4,000) cm-1 with a spectrum resolution of 4 cm^{-1}. The structure and special functional groups of specimens was measured by infrared energy of (2.5–15) μm penetrating substances, to obtain substance-specific absorption spectra.

2.4. *Energy simulation software*

DesignBuilder is an energy simulation that is used to calculate the energy consumption and energy savings for a building. This simulation program is a 3D comprehensive interface built over EnergyPlus, a dynamic calculation model that can simulate building energy consumption and indoor comfort [52]. This study used DesignBuilder to analyze the energy consumptions and energy saving of building applied to the building material with optimized PCMs. To evaluate the PCM, enthalpy-temperature function is required [53], so that the enthalpy properties of the optimized PCMs were analyzed, as well as any other thermal properties.

2.4.1. *Building model description*

The building modelling was selected as residential building, and followed the residential construction standard house established by the Korea Rural Community Corporation, as shown in Fig. 2. The building is (6.0 m × 6.9 m × 3.9 m) (ceiling height of 2.4 m), giving a total floor area of 41.92 m^2. The building is south-oriented, with 30 % window-to-wall area. Considering the boundary conditions, there are the main zone as a living space and the un-conditioned zone as storage. Table 3

shows the construction details of the model, while Table 4 shows the properties of the windows.

Regarding internal heat gains, the model is considered to have the common circulation activity of a residential building. To simulate the actual use of residential building, the schedules of occupancy, lighting, and equipment were set to 100 % running from 18:00 to 08:00 on weekdays, and all day on weekends. The maximum heat gain provided by equipment is 3.00 W/m^2, and the target illumination level is 100 lux. The HVAC conditions were set to "simple HVAC", the basic load calculation algorithms to minimize space heating and cooling loads. Considering set-point temperatures, when the space is occupied, the heating and cooling set-point temperatures are set to (20 and 26) ℃, respectively. When unoccupied, the set-back temperatures of heating and cooling revert to (18 and 28) ℃, respectively, according to the recommendation of the Ministry of Trade, Industry, and Energy of South Korea (MOTIE).

2.4.2. *Climatic conditions*

To evaluate the analysis, the climate conditions in South Korea were those of Gangneung, Gwangju, Incheon, and Ulsan, and Table 5 shows the climate conditions of these cities. The Köppen-Geiger climate classification [54] classifies the general climate of the world into five letters, based on the temperature and precipitation, which are A: equatorial, B: arid, C: warm temperate, D: snow, and E: polar. In addition, further details are divided in small letters based on the temperature and

precipitation. South Korea is located in a humid continental/subtropical climate with dry winter. In summer, the temperature of South Korea is relatively high, and the rainy season produces a lot of rain, especially from July to August. Compared to summer, winter is cold and dry. In addition, the annual difference of temperature is very large. Thus, the specific four districts of South Korea, included in Cfa, Dfa, and Dwa, were selected for energy performance of the optimized PCMs.

3. Analysis of the thermal properties for PCMs

3.1. *PCM optimization*

To investigate the optimized PCM under the thermal comfort range, circulation water bath test was performed under the temperature condition of (15 to 30) ℃, and Figs. 3 (a) and (b) show the results. In the case of the pure PCMs, the phase changes of OT, HT, and HX appeared at ((26–28), (20–22), and (16–18)) ℃, respectively, and it was confirmed that the actual temperature change of these PCMs were observed at the theoretical phase change temperature range of the PCMs. In the case of the mixed PCMs, the phase changes of OTHT, OTHX, and HTHX appeared at ((22–23), (18–20), and (16–18)) ℃, respectively. These mixed PCM were made by mixing each pure PCM at a ratio of 1:1, which indicates that they represent the average values of the phase change temperature range depending on the mixing ratio of the pure PCMs. Thus, according to the thermal comfort range, it was concluded that OTHT with the phase change temperature range of (22–23) ℃ was the optimized PCM. In addition, the circulation water bath test was re-performed depending on the segmentation of

the mixing ratio of OT and HT, as shown in Table 6. The mixed PCMs were divided into five specimens by mixing OT with HT in odd integer ratios of (9:1 to 1:9). The prepared PCMs were named OH91, OH73, OH55, OH37, and OH19, respectively, depending on the mixing ratio. Figures 4 (a) and (b) show the temperature changes of OH91, OH73, OH55, OH37, and OH19 on heating and cooling. The results of circulation water bath showed that the phase changes of OH91, OH73, OH55, OH37, and OH19 appeared at ((24-26), (23-24), (22-23), (21-23), and (20-22)) ℃, respectively. These phase change temperature ranges belonged to the thermal comfort range, and the efficiency of PCMs would be higher due to the segmentation of temperature ranges depending on the PCMs.

3.2. *FTIR analysis and chemical stability of PCMs*

To evaluate the chemical stability of PCMs, FTIR analysis was performed in this study. Figure 5 and Table 7 indicate the FTIR absorption spectra of pure PCM, OT, and HT, and mixed PCMs, the OHs. OT and HT as pure PCMs are *n*-octadecane and *n*-heptadecane, and OHs as mixed PCMs consist of both pure PCMs, including chemical properties according to the alkane chain of *n*-octadecane and *n*-heptadecane. Alkanes, saturated hydrocarbons, consist of hydrogen and carbon atoms, and all bonds are single bonds. Therefore, *n*-octadecane and *n*-heptadecane contained $–CH_2$ and $–CH_3$ bonding, so that OT, HT, and OH indicate only $–CH_2$ and $–CH_3$ bonding peaks in the FTIR spectra. In addition,

as a result of the PCMs, the pure PCMs, OT and HT, have strong wavelengths compared to the OHs. This indicates that the mixed PCMs have lower heat capacity in comparison to the pure PCMs. In addition, FTIR graphs confirmed that the properties of OH do not shift, so that they are not changed after the mixing process. Thus, the characteristics of OH91 to OH19 could be maintained in the structure of pure PCMs due to the physical bonding, without a change in those chemical properties.

3.3. *Thermal properties of PCMs*

To evaluate the properties of PCMs, DSC test was performed. First, Fig. 6 and Table 8 show the DSC curves of OT, HT, and OH55, and the properties of these PCMs. From the curve, OT has only a solid–liquid phase change peak, while HT has both solid–solid and solid–liquid phase change peaks. Thus, OH55, as a mixed PCM with OT and HT, has both solid–solid and solid–liquid phase change peaks. The peaks of OT and HT have narrow widths, which mean the phase change range of OT is narrow, so that it could be helpful to control the target temperature used for TES. However, these two pure PCMs were not included in the thermal comfort range. This indicates that they could not demonstrate perfect phase change, decreasing the efficiency of TES within the thermal comfort range. The phase change peak of OH55 also has a narrow width, but not as narrow as the pure PCMs, which means that OHs can be used by setting the target temperature. In addition, OH55 was included within the thermal comfort range, which means the TES efficiency of OH55 was increased

within the thermal comfort range. The latent heat capacity of OT and HT was (247.6 and 216.7) J/g in the endothermic process, and (245.8 and 213.2) J/g in the exothermic process. There was almost no difference in latent heat between the endothermic and exothermic processes, which means that super-cooling did not occur. The latent heat capacity of OH55 was (171.8 and 156.5) J/g in the endothermic and exothermic processes, respectively. Compared with the pure PCMs, OH55 as mixed PCM showed a difference of latent heat between the endothermic and exothermic processes, so that super-cooling could occur.

Figure 7 and Table 8 show the DSC curves of OH91, OH73, OH55, OH37, and OH19. As mentioned above, the OHs were made by mixing OT and HT, so that they have the characteristics of OT and HT. Those from OH91 to OH19 had a solid–solid phase change peak in the endothermic process as the mixing ratio of HT increased. However, the temperature of the solid–solid phase change peak was decreased with mixing, which means that the phase change peak in the exothermic process was decreased to sub-zero temperature. The latent heat capacity of OH91 to OH19 was measured to be (207.8, 183.2, 171.8, 171.4, and 191.1) J/g in the endothermic process, and (192.0, 194.5, 156.5, 169.0, and 173.6) J/g in the exothermic process, respectively. The differences between the endothermic and exothermic process of OHs were higher than those of the pure PCMs, which means super-cooling could occur, but the difference was insignificant. In addition, according to the

DSC curve, the phase change temperature of OH91 to OH19 was (26.46, 24.47, 24.33, 22.61, and 21.38) ℃ in the endothermic process, and (23.42, 22.39, 20.94, 20.15, and 19.73) ℃ in the exothermic process, respectively, which means that these were included within the thermal comfort range. Therefore, this indicates that OH91 to OH19 could be efficient for energy savings, and could be optimized in the comfort temperature zone.

4. Optimized PCM application

4.1. *Manufacture of gypsum boards mixed with optimized PCMs*

To evaluate the energy savings of the building model applied to the optimized PCMs, the gypsum boards with optimized PCMs were manufactured, being used as the interior finishing materials. The optimized PCMs (OH91, OH73, OH55, OH37, and OH19) were impregnated into the expanded perlite (EP) and vermiculite (EV) to solve the leakage problem and keep their efficient thermal storage quantity, which properties were described in a previous study [55]. Figure 8 shows the procedures of vacuum impregnation of optimized PCMs with EP and EV. EP and EV were merged into the glass filled with optimized PCM (OH91 to OH19), and they were placed in the vacuum oven. They were heated to 60 ℃ in the vacuum oven, and impregnated for 3 h. After that, they were filtered by the filtering process that was described in a previous study [2]. Lastly, EP and EV with a mass of 10 wt% were mixed with gypsum powder, and the gypsum boards with EP (POH) and EV (VOH) were prepared, as shown in Fig. 9.

4.2. *Thermal properties of gypsum boards mixed with optimized PCMs*

To investigate the thermal properties of the gypsum boards with optimized PCMs to simulate the energy performance, thermal conductivity, specific heat capacity, and enthalpy analysis were performed. Figure 10 shows that the thermal conductivities of VOHs were measured to be (0.226, 0.210, 0.199, 0.179, 0.168, 0.155, and 0.138) W/mK, respectively, and the thermal conductivities of POHs were (0.270, 0.261, 0.228, 0.193, 0.175, 0.164, and 0.153) W/mK, respectively. The thermal conductivities of OT and HT were (0.26 and 0.15) W/mK, respectively, which means that the values of specimens increased or decreased, depending on the mixing ratio of OT and HT. In addition, the thermal conductivities of expanded perlite and vermiculite impregnated by OT were (0.23 and 0.15) W/mK [55], respectively, which means that the thermal conductivities of the specimens were influenced by the impregnation amount of PCMs and the thermal characteristics of the expanded perlite and vermiculite as porous materials.

In order to evaluate the energy performance of PCM products, the specific heat capacity and enthalpy of the optimized PCMs were analysed, as shown in Figs. 11 (a) and (b). The average specific heat capacities of OH91 to OH19 were measured to be (1.60, 2.02, 1.33, 1.62, and 2.16) J/gK, respectively. Considering the specific heat capacities of OT and HT on liquid state, those values were (1.53 and 1.93) J/gK, respectively. This means that the specific heat capacities of the

optimized PCMs with higher mixing amount of HT were higher than those with higher mixing amount of OT. Therefore, the highest enthalpy of optimized PCMs was OH19 influenced by the specific heat capacity, even though OH91 had the highest latent heat capacity. In conclusion, Table 9 shows the properties of VOHs and POHs, and those values are used to evaluate the energy performance by simulation.

5. Energy simulation analysis

To simulate the energy performance, the VOHs and POHs were used to replace the gypsum board of external walls in building, and they were analyzed by simulation compared with the building model with the existing gypsum board (REF), as shown in Fig. 12.

5.1. *Energy performance analysis of the model building*

5.1.1. *Gangneung*

Table 10 and Fig. 13 (a) show the monthly cooling and heating energy savings of (VOH91 to VOH19) and (POH91 to POH19) for Gangneung. The building model for Gangneung used cooling energy from April to October, and heating energy from October to May.

In the case of the cooling energy savings of the specimens in Gangneung, the maximum cooling energy savings were shown by OH73, and were measured to be (13.18 and 13.07) kWh for VOH73 and POH73, respectively. On the other hand, the minimum cooling energy savings were shown by OT, and were measured to be (8.83 and 8.77) kWh for VOT and POT, respectively. The phase

change temperatures of OH73 and OT were ((22.39–24.47) and (26.22–29.81)) ℃, respectively, and the average temperature of Gangneung in cooling hardly came close to the phase change temperature of OT. This indicates that the OT resulted in less cooling energy reduction, since it only partially exercised the latent heat storage in the cooling time of Gangneung.

In the case of the heating energy savings, the maximum heating energy savings were shown by OH19, and were measured to be (11.07 and 11.67) kWh for VOH19 and POH19, respectively. On the other hand, the minimum heating energy savings were shown by OT, and were measured to be (4.50 and 5.42) kWh for VOT and POT, respectively. The phase changes of OH19 and OT were ((19.73–21.38) and (26.22–29.81)) ℃, respectively, and the average temperature of Gangneung in heating did not exceed the phase change temperature of OT. This indicates that the OT resulted in less heating energy reduction, since it did not exercise the latent heat storage in the heating time of Gangneung.

5.1.2. *Gwangju*

Table 11 and Fig. 13 (b) show the monthly cooling and heating energy savings of (VOH91 to VOH19) and (POH91 to POH19) for Gwangju. The building model for Gwangju used cooling energy from April to November, and heating energy from October to May.

In the case of the cooling energy savings of the specimens in Gwangju, the maximum cooling energy

savings were shown by OH73, and were measured to be (11.10 and 10.89) kWh for VOH73 and POH73, respectively. On the other hand, the minimum cooling energy savings were shown by OT, and were measured to be (8.83 and 8.77) kWh for VOT and POT, respectively. The phase change temperatures of OH73 and OT were ((22.39–24.47) and (26.22–29.81)) ℃, respectively, and the average temperature of Gwangju in cooling hardly came close to the phase change temperature of OT. This indicates that the OT resulted in less cooling energy reduction, since it only partially exercised the latent heat storage in the cooling time of Gwangju.

In the case of the heating energy savings, the maximum heating energy savings were shown by OH19, and were measured to be (10.07 and 10.59) kWh for VOH19 and POH19, respectively. On the other hand, the minimum heating energy savings were shown by OT, and were measured to be (3.97 and 4.75) kWh for VOT and POT, respectively. The phase changes of OH19 and OT were ((19.73–21.38) and (26.22–29.81)) ℃, and the average temperature of Gwangju in heating did not exceed the phase change temperature of OT. This indicates that the OT resulted in less heating energy reduction, since it did not exercise the latent heat storage in the heating time of Gwangju.

5.1.3. *Incheon*

Table 12 and Fig. 13 (c) show the monthly cooling and heating energy savings of (VOH91 to VOH19) and (POH91 to POH19) for Incheon. The building model for Incheon used cooling energy

from May to October, and heating energy from October to May.

In the case of the cooling energy savings of the specimens in Incheon, the maximum cooling energy savings were shown by OH73, and were measured to be (8.22 and 8.13) kWh for VOH73 and POH73, respectively. On the other hand, the minimum cooling energy savings were shown by OT, and were measured to be (5.45 and 5.41) kWh for VOT and POT, respectively. The phase change temperatures of OH73 and OT were ((22.39–24.47) and (26.22–29.81)) ℃, respectively, and the average temperature of Incheon in cooling hardly came close to the phase change temperature of OT. This indicates that the OT resulted in less cooling energy reduction, since it only partially exercised the latent heat storage in the cooling time of Incheon.

In the case of the heating energy savings, the maximum heating energy savings were shown by OH19, and were measured to be (3.82 and 4.08) kWh for VOH19 and POH19, respectively. On the other hand, the minimum heating energy savings were shown by OT, and were measured to be (1.39 and 2.17) kWh for VOT and POT, respectively. The phase changes of OH19 and OT were ((19.73–21.38) and (26.22–29.81)) ℃, respectively, and the average temperature of Incheon in heating did not exceed the phase change temperature of OT. This indicates that the OT resulted in less heating energy reduction, since it did not exercise the latent heat storage in the heating time of Incheon.

5.1.4. *Ulsan*

Table 13 and Fig. 13 (d) show the monthly cooling and heating energy savings of (VOH91 to VOH19) and (POH91 to POH19) for Ulsan. The building model for Ulsan used cooling energy from April to December, and heating energy from October to May.

In the case of the cooling energy savings of the specimens in Ulsan, the maximum cooling energy savings were shown by OH73, and were measured to be (12.15 and 12.01) kWh for VOH73 and POH73, respectively. On the other hand, the minimum cooling energy savings were shown by OT, and were measured to be (8.04 and 7.89) kWh for VOT and POT respectively. The phase change temperatures of OH73 and OT were ((22.39–24.47) and (26.22–29.81)) ℃, and the average temperature of Ulsan in cooling hardly came close to the phase change temperature of OT. This indicates that the OT resulted in less cooling energy reduction, since it only partially exercised the latent heat storage in the cooling time of Ulsan.

In the case of the heating energy savings, the maximum heating energy savings were shown by OH19, and were measured to be (12.43 and 13.04) kWh for VOH19 and POH19, respectively. On the other hand, the minimum heating energy savings were shown by OT, and were measured to be (4.73 and 5.62) kWh for VOT and POT, respectively. The phase changes of OH19 and OT were ((19.73–21.38) and (26.22–29.81)) ℃, respectively, and the average temperature of Ulsan in heating did not exceed the phase change temperature of OT. This indicates that the OT resulted in less

heating energy reduction, since it did not exercise the latent heat storage in the heating time of Ulsan.

5.2. *Discussions*

According to the energy simulation results of the building model with optimized PCMs, the most optimized PCM is OH73 in cooling and OH19 in heating, as shown in Fig. 14. In the case of the monthly energy savings in the cities, the energy savings in winter were increased in most cities, but Incheon used more heating energy in heating when the PCMs were applied to the building, as shown in Fig. 14 (c). This means that the PCMs did not play a role as thermal storage materials, since the temperature of winter in Incheon mostly maintains sub-zero temperature. In addition, according to the phase change temperature of the optimized PCMs, OT could invoke the highest energy consumption in winter. However, the highest energy use was for OH73. Since the specific heat capacity and thermal conductivity of OH73 are higher than those of the others, OH73 used more heating energy consumption in heating than the other PCMs; the average specific heat capacity of (OH91 to OH19) is (1.60, 2.02, 1.33, 1.62, and 2.16) J/gK, respectively. As a result of the total energy savings of the cities, Ulsan demonstrated the highest energy savings. This is because the climate of Ulsan did not drop below zero temperature for most of the day in winter. This means that the average temperature of Ulsan relatively maintained a higher annual temperature than the others. Thus, PCM is considered to be more effective in hot regions.

According to the energy savings of the specimens applied to the building, the energy savings of VOH were higher in cooling, while POH had higher energy savings in heating, as shown in Fig. 14. The greatest difference of VOH and POH is in thermal conductivity, which means that the thermal properties of the expanded vermiculite and perlite were different, and influenced the energy performance. In addition, the difference of energy savings in heating and cooling was considered to be the difference between the indoor and outdoor temperature, as shown in Fig. 15, in which T_{int} and T_{ext} represent the indoor and outdoor temperature, while SF_{int} and SF_{ext} represent the inside and outside surface temperature, respectively. Figure 15 (a) shows the indoor and outdoor temperature of the building in the hottest day of summer. The difference between indoor and outdoor temperature in summer is not large; the outdoor temperature in the afternoon is higher than the indoor temperature. Thus, as the heat flows from the outside to the inside as shown in Fig. 15 (b), POH becomes thermally unfavourable. In contrast, the indoor temperature in winter is always higher than the outdoor temperature, as shown in Fig. 15 (c), so that the heat flows from the inside to the outside, as shown in Fig. 15 (d). Therefore, POH with higher thermal conductivities than VOH is considered to be efficient in winter, since higher thermal conductivities led to the efficient phase change of PCMs, compared to the heat flows to the outside. Consequently, in order to improve the usability of the optimized PCMs within the comfort temperature, it is confirmed that there are many variables to

consider, such as phase change temperature, specific heat capacity, latent heat capacity, thermal conductivity, and climate conditions.

6. Conclusion

The optimized PCMs under the thermal comfort range were manufactured, and analyzed by energy simulation in the climate conditions of South Korea. First, *n*-octadecane (OT), *n*-heptadecane (HT), and *n*-hexadecane (HX) were selected to manufacture the optimized PCMs that were close to the thermal comfort range. Those PCMs were divided into various types of mixing ratio, and were analyzed by circulation water bath test. As a result, mixed PCMs of OT and HT having phase change temperature of (22–23) ℃ were suitable for the thermal comfort range. In addition, the mixing ratios of OT and HT were divided into odd integer (9:1 to 1:9) ratios of OT and HT of (OH91, OH73, OH55, OH37, and OH19), and their thermal properties analyzed. As a result of the thermal properties, the phase change temperatures of (OH91 to OH19) were found to be ((23.46–26.46), (24.47–22.39), (24.33–20.94), (22.61–20.15), and (21.38–19.73)) ℃, respectively, and the latent heat capacities of (OH91 to OH19) were (207.8, 183.2, 171.8, 171.4, and 191.1) J/g in the endothermic process, and (194.5, 192.0, 156.5, 169.0, and 173.6) J/g in the exothermic process, respectively.

To evaluate the energy performance of the prepared PCMs, the PCMs were impregnated into expanded perlite (EP) and vermiculite (EV). In addition, the gypsum boards mixed with EP and EV

were manufactured to replace the conventional gypsum board (REF) in the wall layers of the building model established by the Korea Rural Community Corporation. The climate conditions of Gangneung, Gwangju, Incheon, and Ulsan in South Korea were selected. As a result of the energy performance, OH73 had the maximum energy savings in cooling, and OH19 in heating. The maximum total annual energy savings were shown by OH73, which means OH73 was the best optimized PCMs for the climate of South Korea. The results of this study confirmed that the efficiencies of the PCMs optimized in the specific climates under the thermal comfort range were based on the materials for impregnation, and the thermal conductivity, which led to energy savings in summer and winter. In addition, the cooling energy savings of PCMs were higher than the heating energy savings, which means the TES of PCMs were efficient in hot climates. Thus, it seems that it is necessary to continue such further studies in the future.

References

[1] Wi S, Jeong S, Chang SJ, Lee J, Kim S. Evaluation of energy efficient hybrid hollow plaster panel using phase change material / xGnP composites. Appl Energy 2017;205:1548–59.

[2] Lee J, Wi S, Jeong S, Chang SJ, Kim S. Development of thermal enhanced *n*-octadecane/porous nano carbon-based materials using 3-step filtered vacuum impregnation method. Thermochim Acta 2017;655:194–201.

[3] Jeon J, Jeong S, Lee J, Seo J, Kim S. High thermal performance composite PCMs loading xGnP for application to building using radiant floor heating system. Sol Energy Mater Sol Cells 2015;101:51-56.

[4] Cabeza LF, Martorell I, Miró L, Fernández AI, Barreneche C. 1: Introduction to thermal energy storage (TES) systems. Editor(s): Cabeza LF. Adv Therm Energy Storage Syst. Woodhead Publishing. 2015. p. 1–28

[5] Solé A, Martorell I, Cabeza LF. State of the art on gas–solid thermochemical energy storage systems and reactors for building applications. Renew Sustain Energy Rev 2015;47:386–98

[6] de Gracia A, Cabeza LF. Phase change materials and thermal energy storage for buildings. Energy Build. 2015;103:414–9

[7] Wang L, Meng D. Fatty acid eutectic/polymethyl methacrylate composite as formstable phase change material for thermal energy storage. Appl Energy 2010;87:2660–5.

[8] Wang Y, Liang D, Liu F, Zhang W, Di X, Wang C. A polyethylene glycol/hydroxyapatite composite phase change material for thermal energy storage. Appl Therm Eng 2017;113:1475–82.

[9] Zhang H, Gao X, Chen C, Xu T, Fang Y, Zhang Z. A capric–palmitic–stearic acid ternary eutectic mixture/expanded graphite composite phase change material for thermal energy storage. Compos Part A: Appl Sci Manuf 2016;87:138–45.

[10] Jeong S, Chang SJ., Wi S, Kang Y, Lim J, Chang JD, et al. Energy efficient concrete with n-octadecane/xGnP SSPCM for energy conservation in infrastructure. Constr Build Mater 2016;106:543–9.

[11] Waqas A. Din Z. U. Phase change material (PCM) storage for free cooling of buildings – a review. Renew Sustain Energy Rev 2013;18:607-625.

[12] Souayfane F., Fardoun F., Biwole P.H. Phase change materials (PCM) for cooling applications in buildings: a review. Energy Build 2016:129;396-431.

[13] Fukai J., Kanou M., Kodama Y., Miyatake O. Thermal conductivity enhancement of energy storage media using carbon fibers. Energy Convers Manage:2000:41;1543-1556.

[14] Baetens R, Jelle BP, Gustavsen A. Phase change materials for building applications: a state-of-the-art review. Energy Build 2010;42:1361–8.

[15] Tyagi VV, Buddhi D. PCM thermal storage in buildings: a state of art. Renew Sustain Energy Rev 2007;11:1146–66.

[16] Fauzi H, Metselaar HS, Mahlia T, Silakhori M. Sodium laurate enhancements the thermal properties and thermal conductivity of eutectic fatty acid as phase change material (PCM). Sol Energy 2014;102:333–7.

[17] Jeong SG, Chang SJ, Wi S, Kang Y, Lim JH, Chang JD, Kim S. Energy efficient concrete with n-octadecane/xGnP SSPCM for energy conservation in infrastructure. Constr Build Mater 2016;106:543–9.

[18] Mu M, Basheer PAM, Sha W, Bai Y, McNally T. Shape stabilised phase change materials based on a high melt viscosity HDPE and paraffin waxes. Appl Energy 2016;162:68–82.

[19] Jeong S, Chang SJ, Wi S, Kang Y, Lee H, Kim S. Development of heat storage gypsum board with paraffin-based mixed SSPCM for application to buildings. J Adhes Sci Technol 2017;31:297–309.

[20] Lee H, Jeong S, Chang SJ, Kang Y, Wi S, Kim S. Thermal performance evaluation of fatty acid ester and paraffin based mixed SSPCMs using exfoliated graphite nanoplatelets (xGnP). Appl Sci 2016;6:106.

[21] Kang Y, Jeong S, Wi S, Kim S. Energy efficient Bio-based PCM with silica fume composites to apply in concrete for energy saving in buildings. Sol Energy Mater Sol Cells 2015;143:430–4.

[22] Wi S, Seo J, Jeong S, Chang SJ, Kang Y, Kim S. Thermal properties of shape-stabilized phase change materials using fatty acid ester and exfoliated graphite nanoplatelets for saving energy in buildings. Sol Energy Mater Sol Cells 2015;143:168–73.

[23] Chung O, Jeong S, Kim S. Preparation of energy efficient paraffinic PCMs/expanded vermiculite and perlite composites for energy saving in buildings. Sol Energy Mater Sol Cells 2015;137:107–12.

[24] Jeong S, Lee J, Seo J, Kim S. Thermal performance evaluation of Bio-based shape stabilized PCM with boron nitride for energy saving. Int J Heat Mass Transf 2014;71:245–50.

[25] Li M, Jin B, Ma Z, Yuan F. Experimental and numerical study on the performance of a new high- temperature packed-bed thermal energy storage system with macroencapsulation of molten salt phase change material. Appl Energy 2018;221:1–15.

[26] Lashgari S, Arabi H, Reza A, Ambrogi V. Thermal and morphological studies on novel PCM microcapsules containing n-hexadecane as the core in a flexible shell. Appl Energy 2017;190:612–22.

[27] Alva G, Huang X, Liu L, Fang G. Synthesis and characterization of microencapsulated myristic acid – palmitic acid eutectic mixture as phase change material for thermal energy storage. Appl Energy 2017;203:677–85.

[28] Wang T, Wang S, Luo R, Zhu C, Akiyama T, Zhang Z. Microencapsulation of phase change materials with binary cores and calcium carbonate shell for thermal energy storage. Appl Energy 2016;171:113–9.

[29] Yu S, Wang X, Wu D. Microencapsulation of n -octadecane phase change material with calcium carbonate shell for enhancement of thermal conductivity and serving durability : Synthesis , microstructure , and performance evaluation. Appl Energy 2014;114:632–43.

[30] Memon SA, Cui H, Zhang H, Xing F. Utilization of macro encapsulated phase change materials for the development of thermal energy storage and structural lightweight aggregate concrete. Appl Energy 2015;139:43–55.

[31] Cui H, Tang W, Qin Q, Xing F, Liao W, Wen H. Development of structural-functional integrated energy storage concrete with innovative macro-encapsulated PCM by hollow steel ball. Appl Energy 2017;185:107–18.

[32] Chang SJ, Kang Y, Wi S, Jeong S, Kim S. Hygrothermal performance improvement of the Korean wood frame walls using macro-packed phase change materials (MPPCM). Appl Therm Eng 2017;114:457–65.

[33] Navarro L, de Gracia A, Castell A, Álvarez S, Cabeza LF. PCM incorporation in a concrete core slab as a thermal storage and supply system: proof of concept. Energy Build 2015;103:70–82.

[34] Soares N, Gaspar A, Santos P, Costa J. Multi-dimensional optimization of the incorporation of PCM-drywalls in lightweight steel-framed residential buildings in different climates. Energy Build 2014;70:411–21.

[35] Souayfane F, Fardoun F, Biwole P. Phase change materials (PCM) for cooling applications in buildings: a review. Energy Build 2016;129:396–431.

[36] Goia F, Perino M, Serra V. Improving thermal comfort conditions by means of PCM glazing systems. Energy Build 2013;60:442–52.

[37] Evola G, Marletta L, Sicurella F. A methodology for investigating the effectiveness of PCM wallboards for summer thermal comfort in buildings. Build Environ 2013;59:517–27.

[38] Evola G, Marletta L, Sicurella F. Simulation of a ventilated cavity to enhance the effectiveness of PCM wallboards for summer thermal comfort in buildings. Energy Build 2014;70:480–9.

[39] Nghana B, Tariku F. Phase change material's (PCM) impacts on the energy performance and thermal comfort of buildings in a mild climate. Build Environ 2016;99:221–38.

[40] Figueiredo A, Vicente R, Lapa J, Cardoso C, Rodrigues F. Indoor thermal comfort assessment using different constructive solutions incorporating PCM. Appl Energy 2017;208:1208–21.

[41] Marin P, Saffari M, Gracia A De, Zhu X, Farid MM, Cabeza LF, et al. Energy savings due to the use of PCM for relocatable lightweight buildings passive heating and cooling in different weather conditions. Energy Build 2016;129:274–83.

[42] Cascone Y, Capozzoli A, Perino M. Optimisation analysis of PCM-enhanced opaque building envelope components for the energy retro fitting of office buildings in Mediterranean climates. Appl Energy 2018;211:929–53.

[43] Jamil H, Alam M, Sanjayan J, Wilson J. Investigation of PCM as retrofitting option to enhance occupant thermal comfort in a modern residential building. Energy Build 2016;133:217-229.

[44] Chang SJ, Wi S, Jeong S, Kim S. Thermal performance evaluation of macro-packed phase change materials (PCMs) using heat transfer analysis device. Energy Build 2016;117:120–7.

[45] International Standard, ISO 13790 – Energy performance of buildings – Calculation of energy use for space heating and cooling, 2008.

[46] Kim S, Chang SJ, Chung O, Jeong S, Kim S. Thermal characteristics of mortar containing hexadecane / xGnP SSPCM and energy storage behaviors of envelopes integrated with enhanced heat storage composites for energy efficient buildings. Energy Build 2014;70:472–9.

[47] Chang SJ, Wi S, Jeong S, Kim S. Analysis on phase transition range of the pure and mixed phase change materials (PCM) using a circulation chamber test and differentiation. J Therm Anal Calorim 2018;131:1999–2004.

[48] Jeong S, Chang SJ, Wi S, Kang Y, Kim S, Jeong S, et al. Development of heat storage gypsum board with paraffin-based mixed SSPCM for application to buildings. J Adhes Sci Technol 2017;31:297-309.

[49] Jeong SG, Jeon J, Seo J, et al. Performance evaluation of the microencapsulated PCM for woodbased flooring application. Energy Convers. Manage. 2012;64:516–521.

[50] Jin Xing, Xiaodong Xu, Zhang Xiaosong, Yin Yonggao. Determination of the PCM melting temperature range using DSC. Thermochim Acta 2014;595:17–21.

[51] Cha J, Seo J, Kim S. Building materials thermal conductivity measurement and correlation with heat flow meter, J Therm Anal Calorim 2012:109:295-300.

[52] Zhang A, Bokel R, Dobbelsteen A Van Den, Sun Y, Huang Q, Zhang Q. An integrated school and schoolyard design method for summer thermal comfort and energy efficiency in Northern China. Build Environ 2017;124:369–87.

[53] Konstantinidou CA, Lang W, Papadopoulos AM. Multiobjective optimization of a building envelope with the use of phase change materials (PCMs) in Mediterranean climates. Int J Energy Res 2018:1–18.

[54] Kottek M, Grieser J, Beck C, Rudolf B, Rubel F. World Map of the Köppen-Geiger climate classification updated. Meteorol Zeitschrift 2006;15:259-63.

[55] Chung O, Jeong S, Kim S. Solar Energy Materials & Solar Cells Preparation of energy efficient paraffinic PCMs / expanded vermiculite and perlite composites for energy saving in buildings. Sol Energy Mater Sol Cells 2015;137:107–12.

Figures

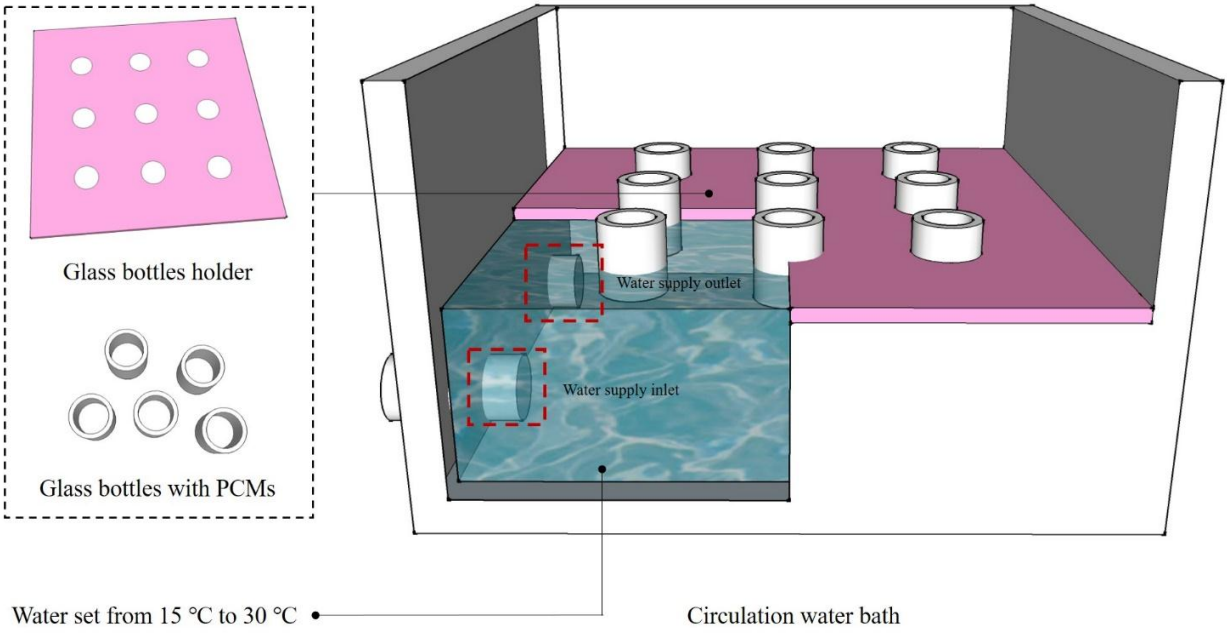

Figure 1. Schematic of circulation water bath test.

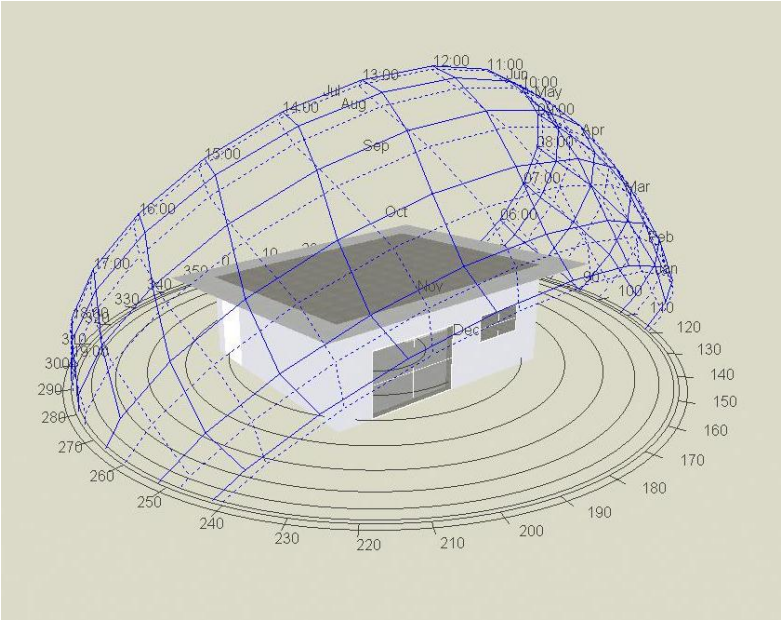

Figure 2. Building modelling by the Korea Rural Community Corporation.

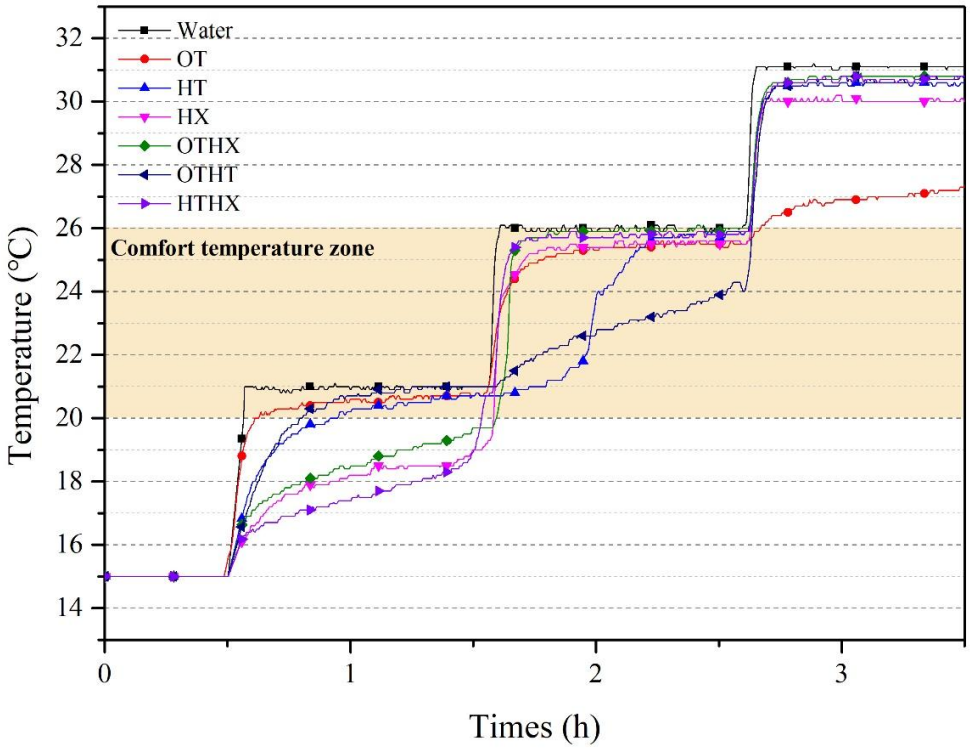

(a) Heating.

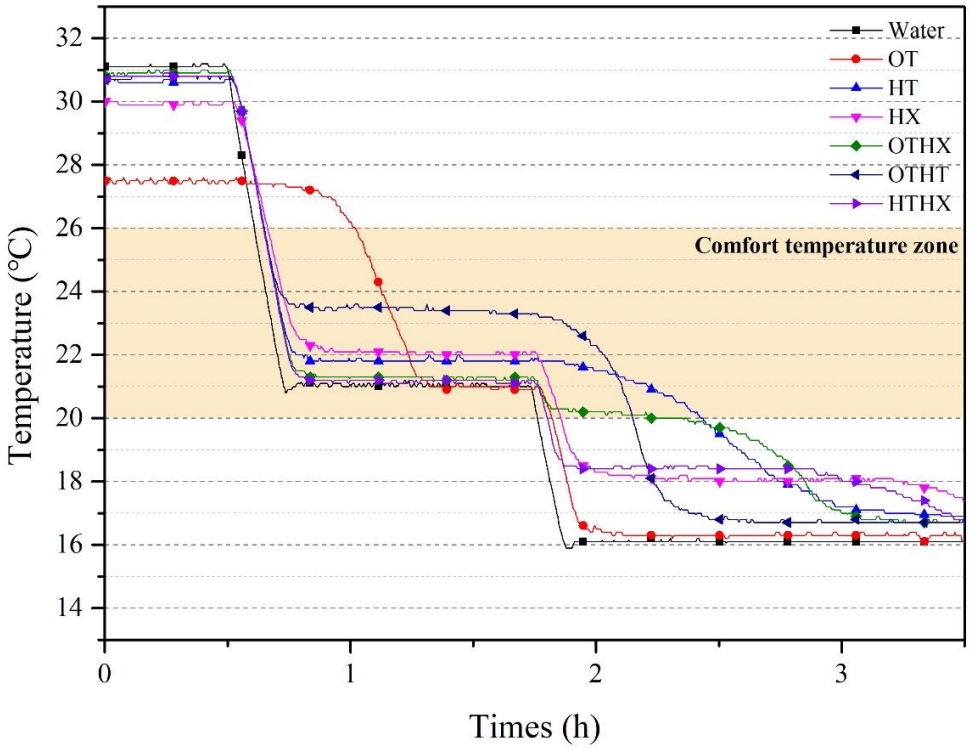

(b) Cooling.

Figure 3. Temperature changes of PCMs on (a) heating, and (b) cooling.

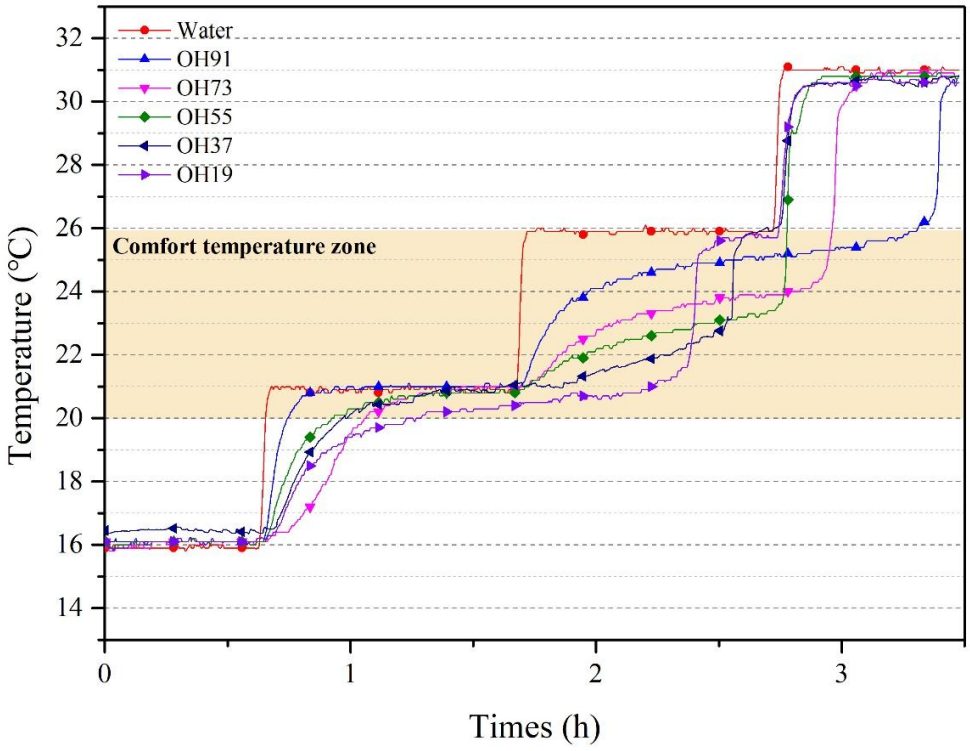

(a) Heating.

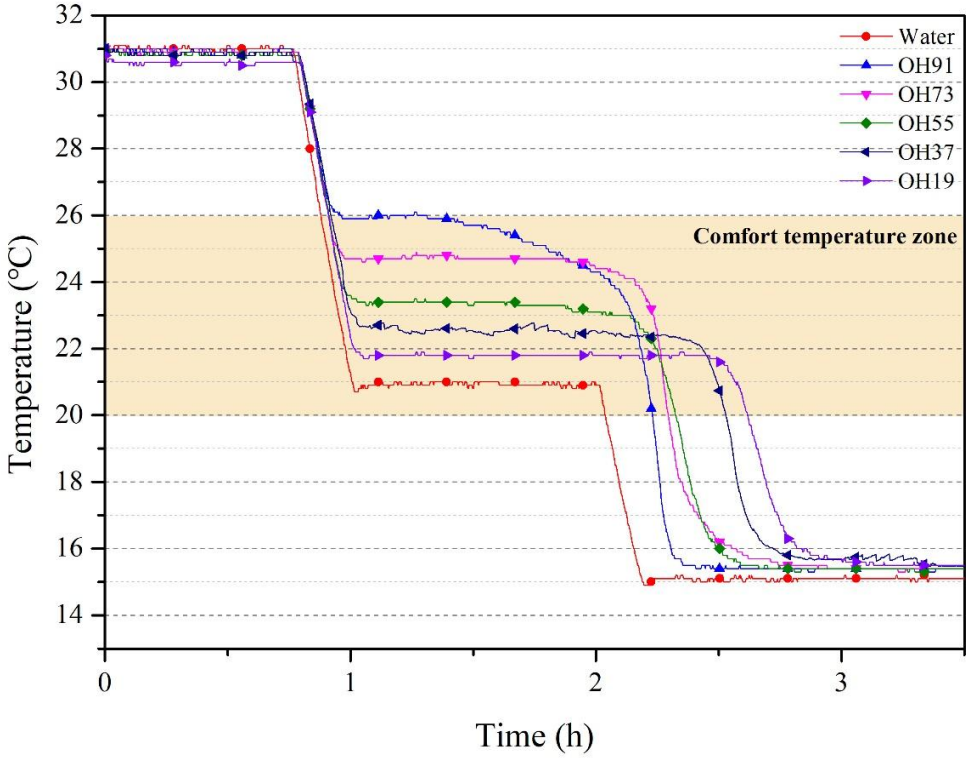

(b) Cooling.

Figure 4. Temperature changes of OH91 to OH19 on (a) heating, and (b) cooling.

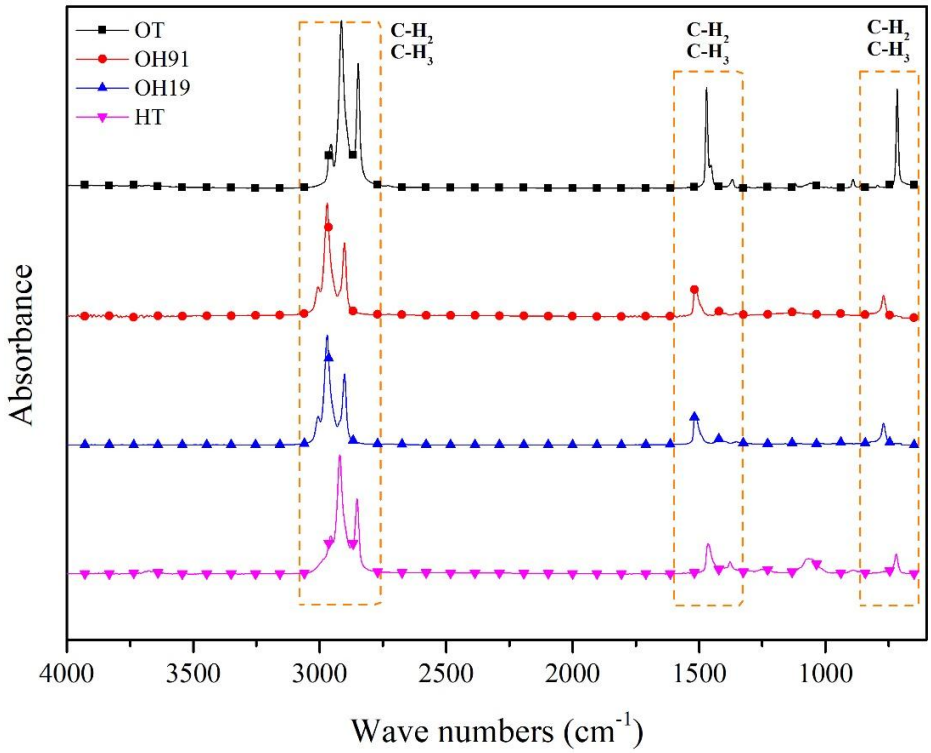

Figure 5. FTIR spectra of OT, OHs, and HT.

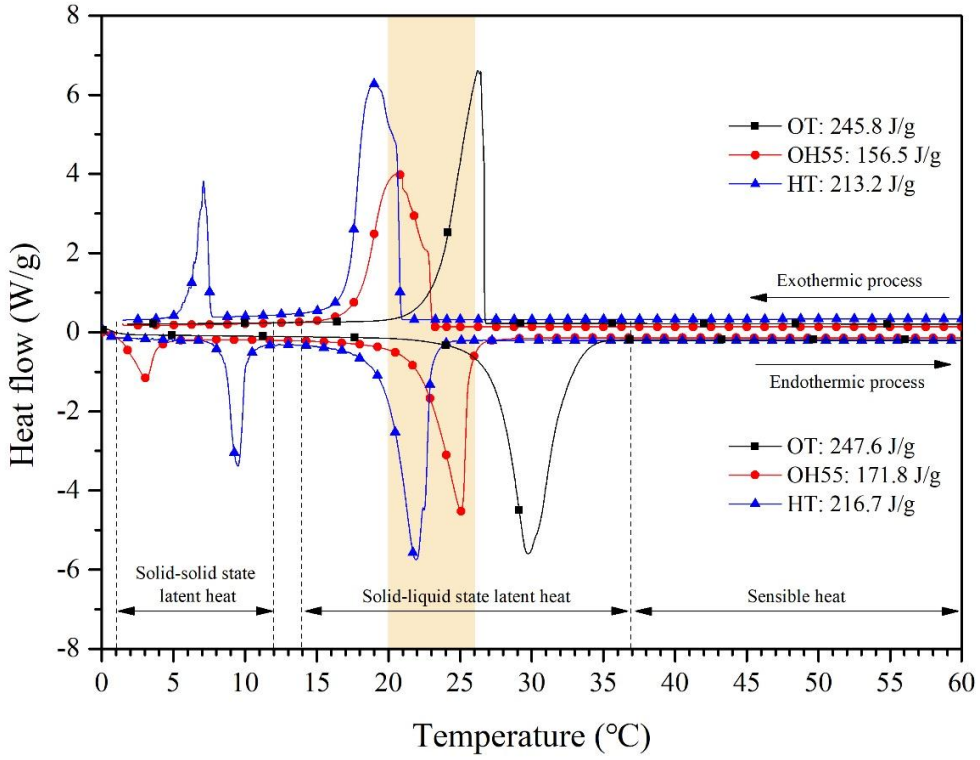

Figure 6. DSC curves of OT, OHs, and HT.

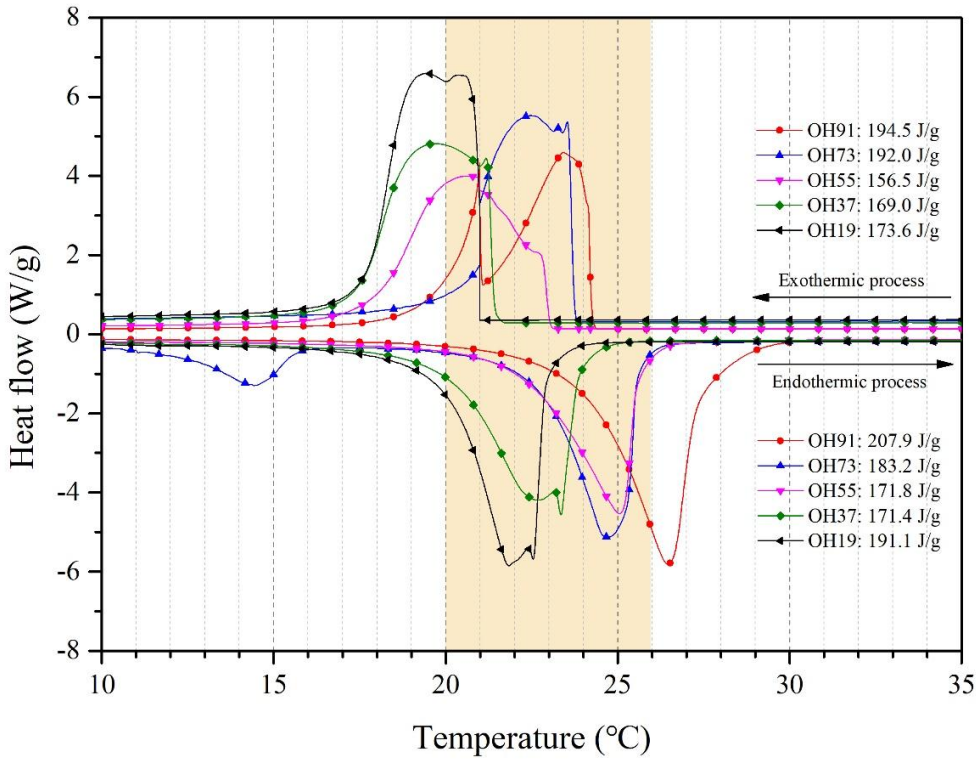

Figure 7. DSC curves of (OH91 to OH19).

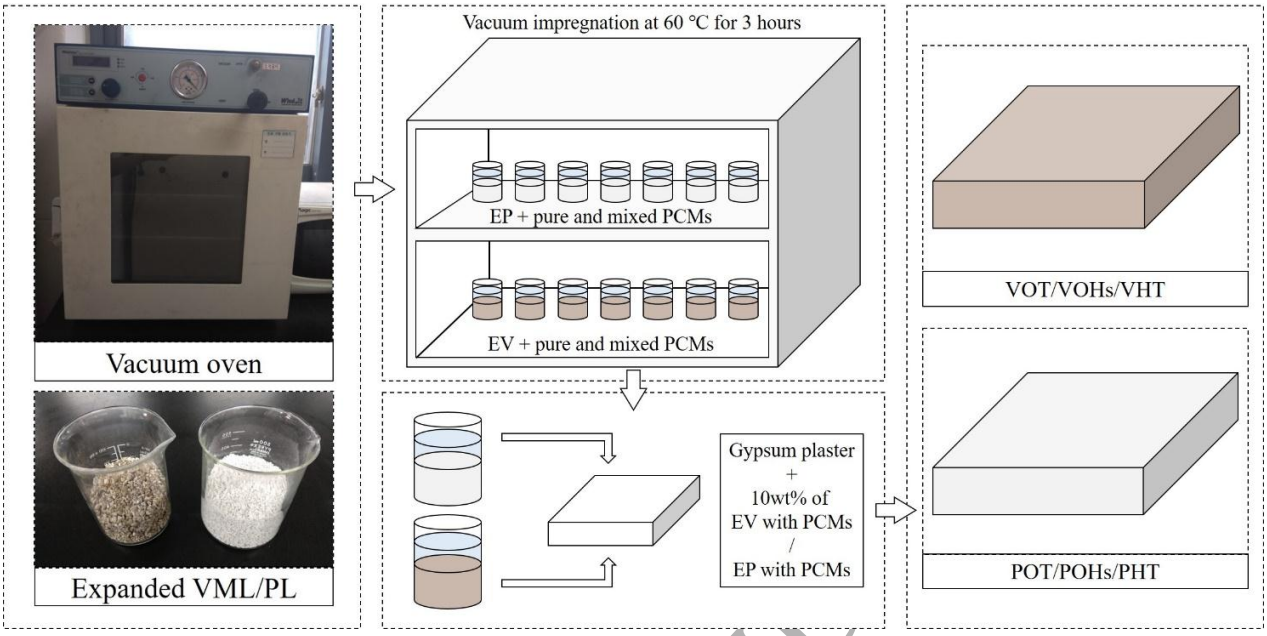

Figure 8. Schematic of the manufacture of the gypsum board with EV and EP impregnated by PCMs.

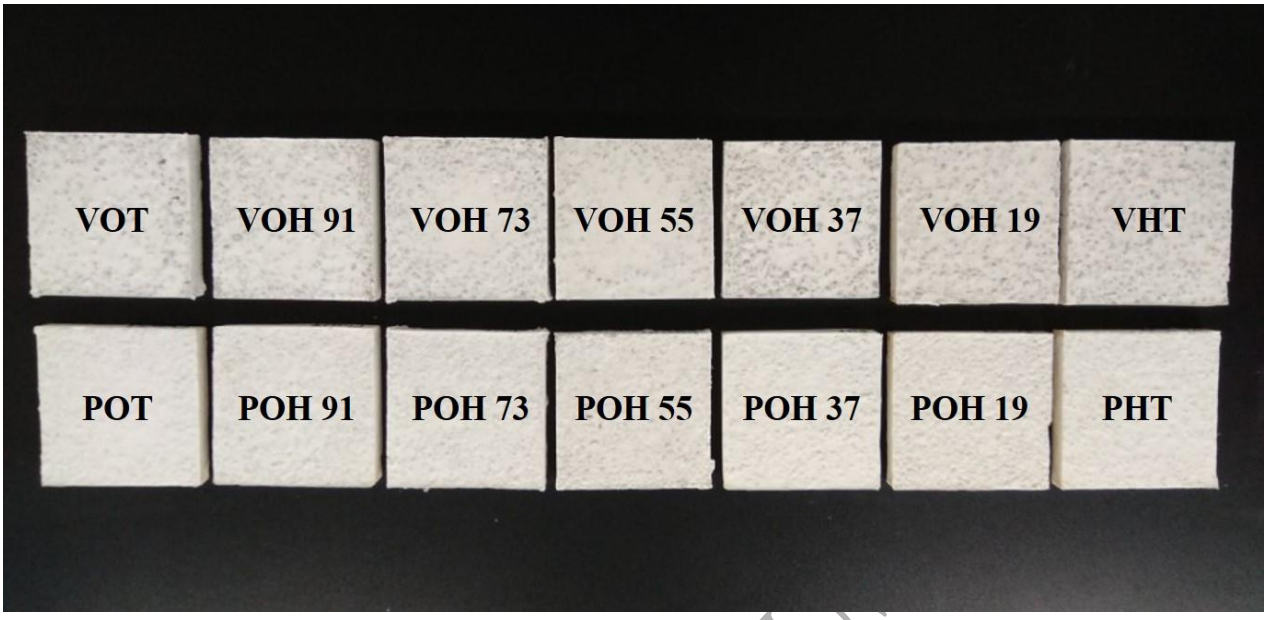

Figure 9. Actual images of the gypsum board with EV and EP impregnated by OT, HT, and (OH91 to OH19).

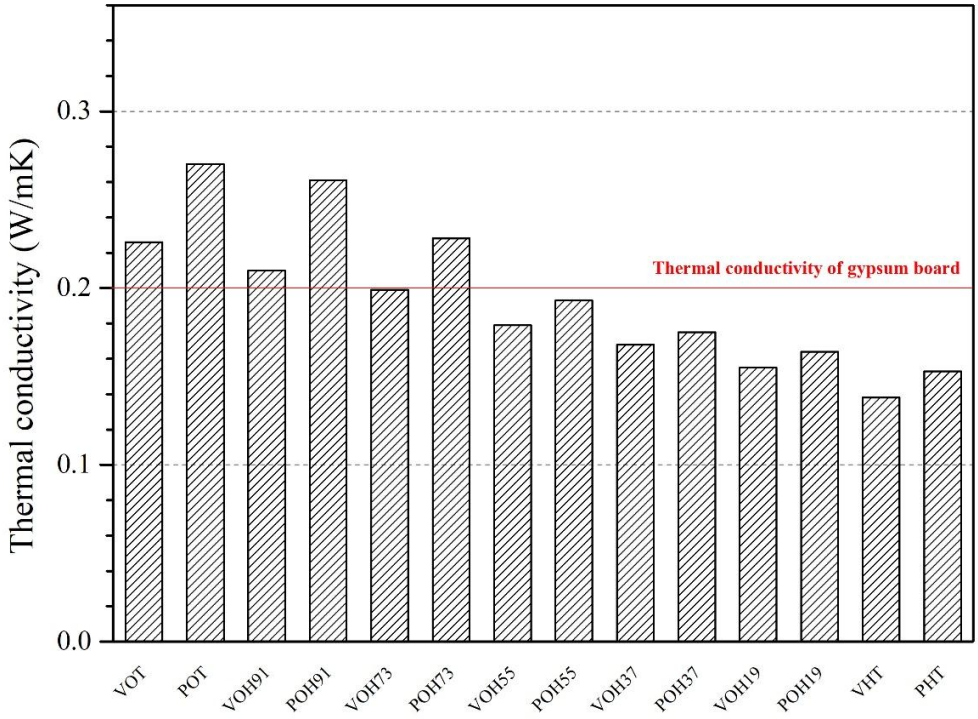

Figure 10. Thermal conductivities of VOT, VOHs, VHT, POT, POHs, and PHT.

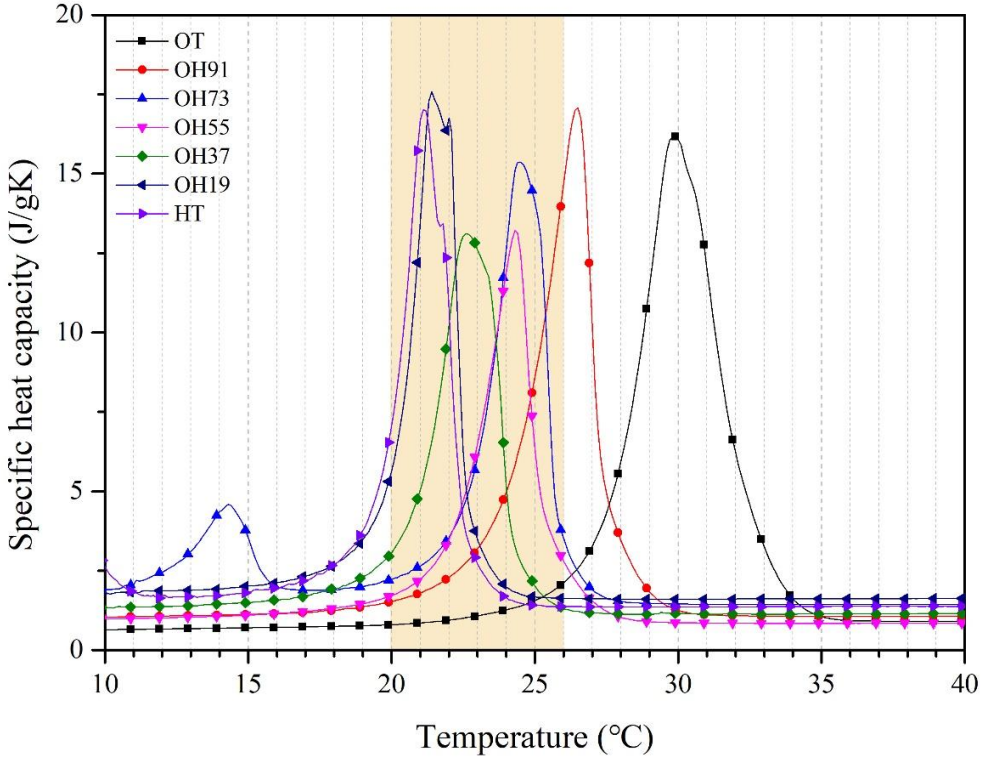

(a) Average specific heat capacities of specimens.

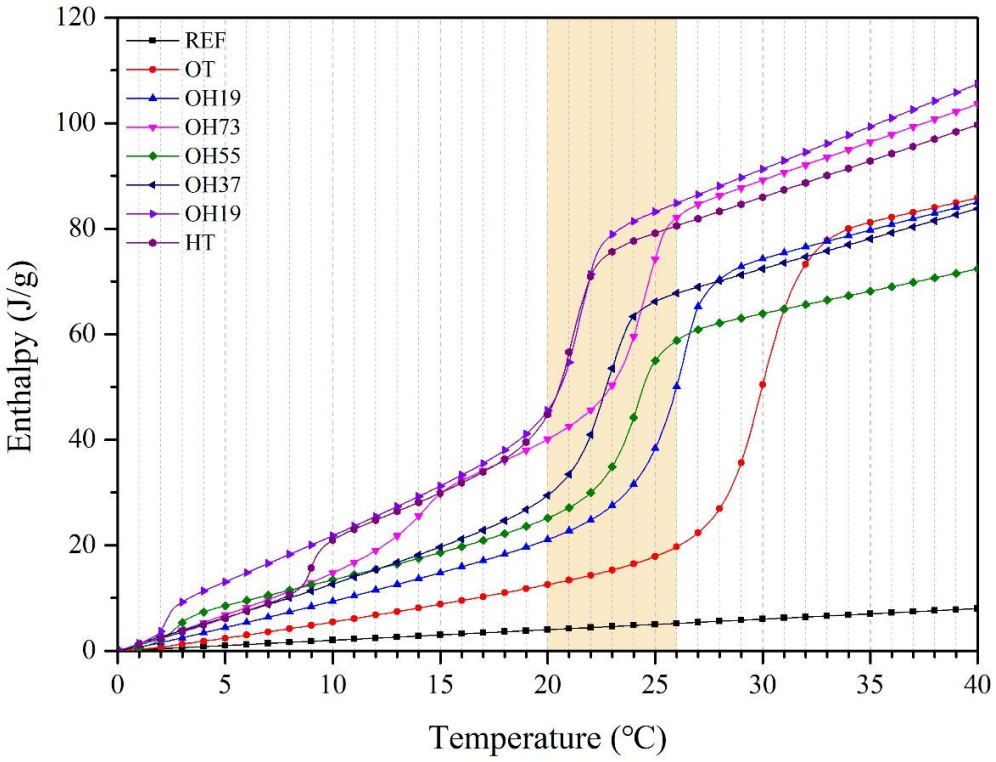

(b) Enthalpy of specimens.

Figure 11. (a) Average specific heat capacities, and (b) enthalpy of VOT, VOHs, VHT, POT, POHs, and PHT.

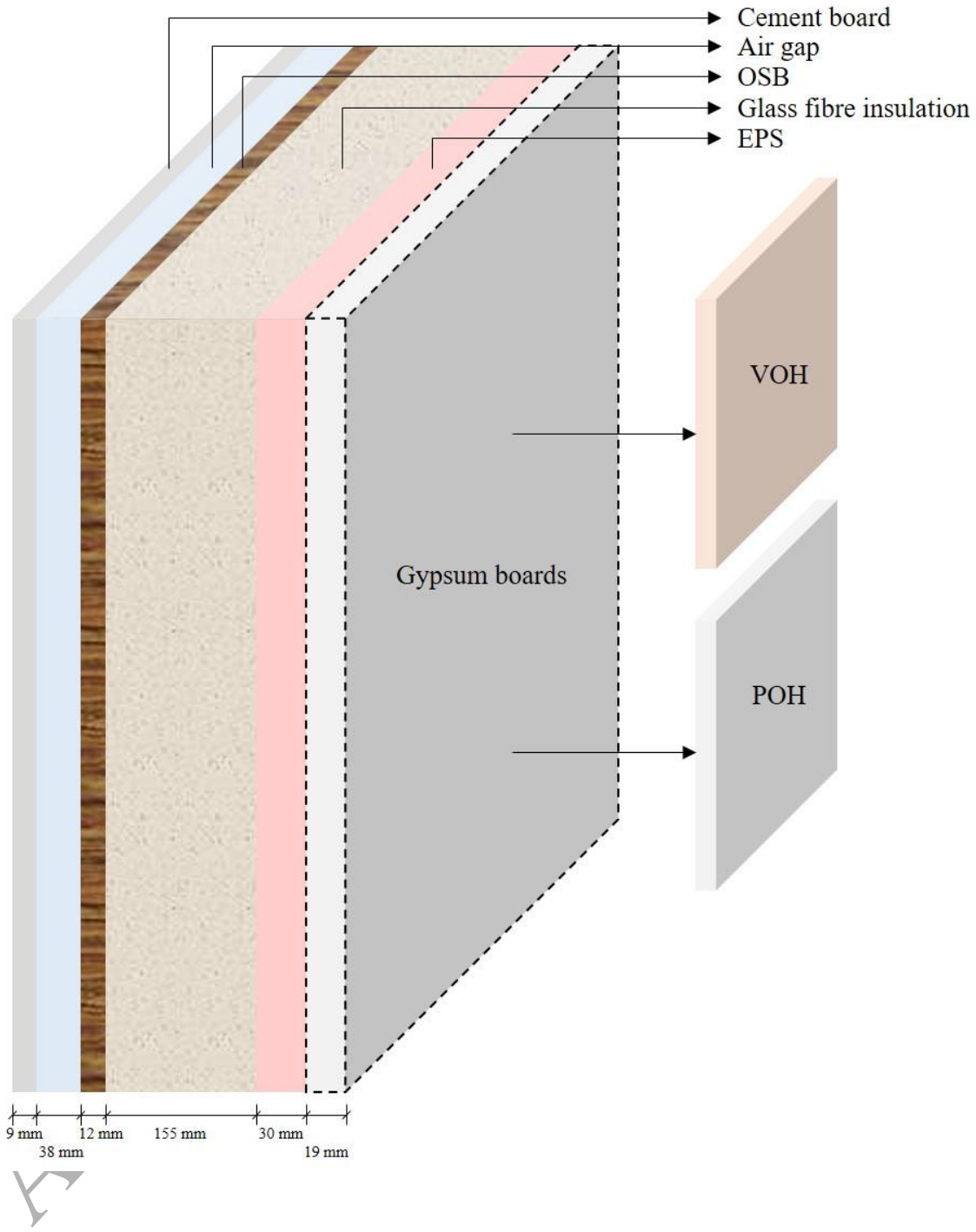

Figure 12. Assembly of walls in the building model.

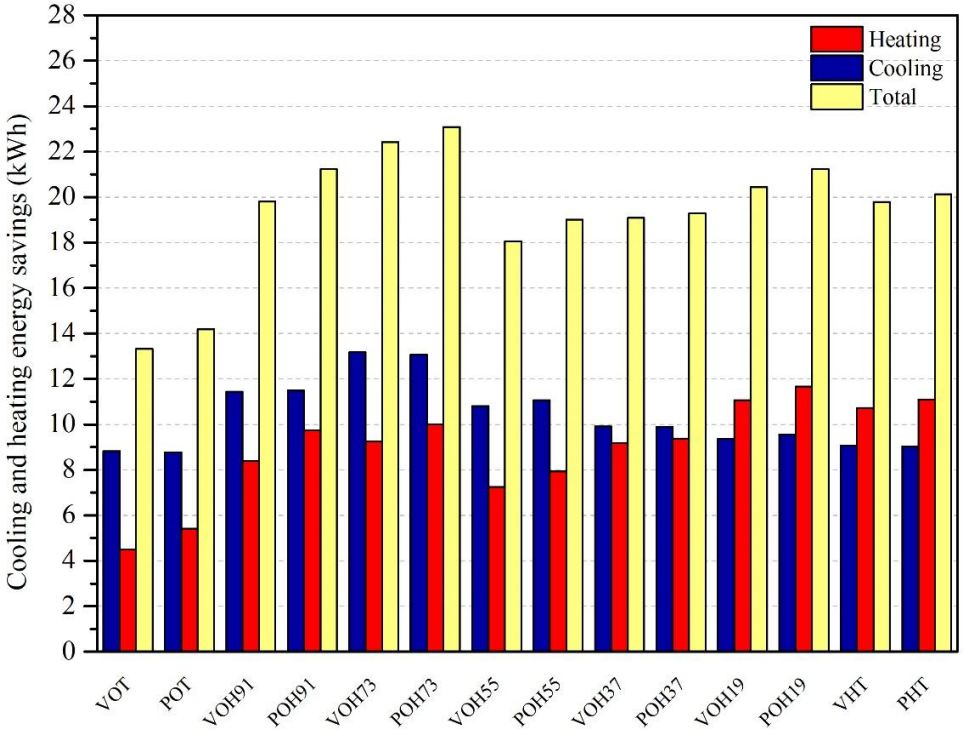

(c) Gangneung.

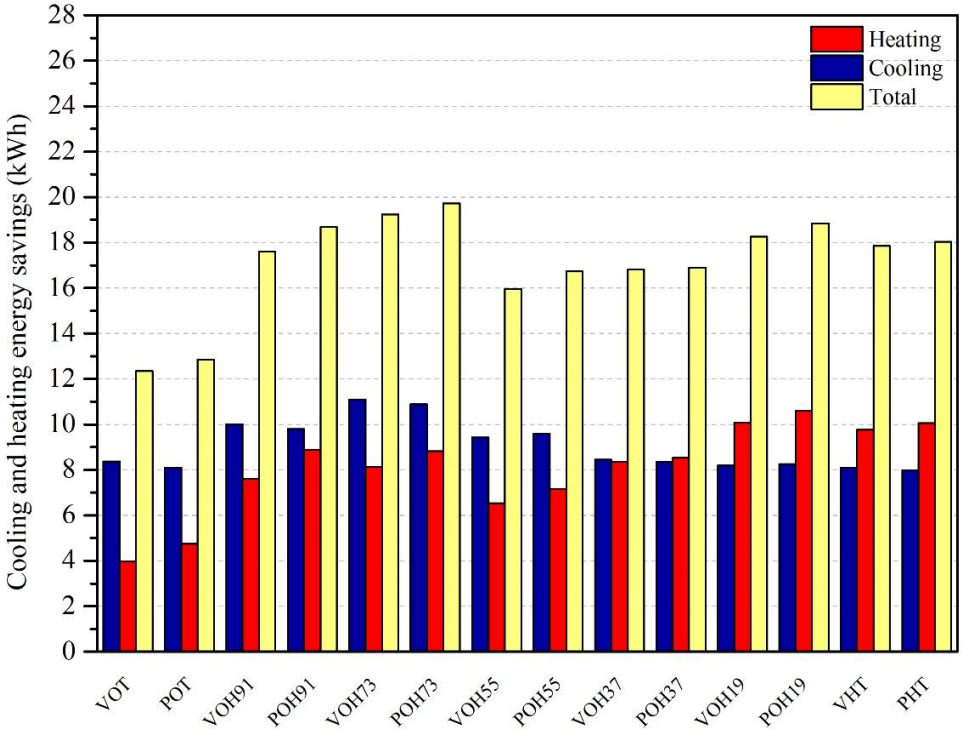

(d) Gwangju.

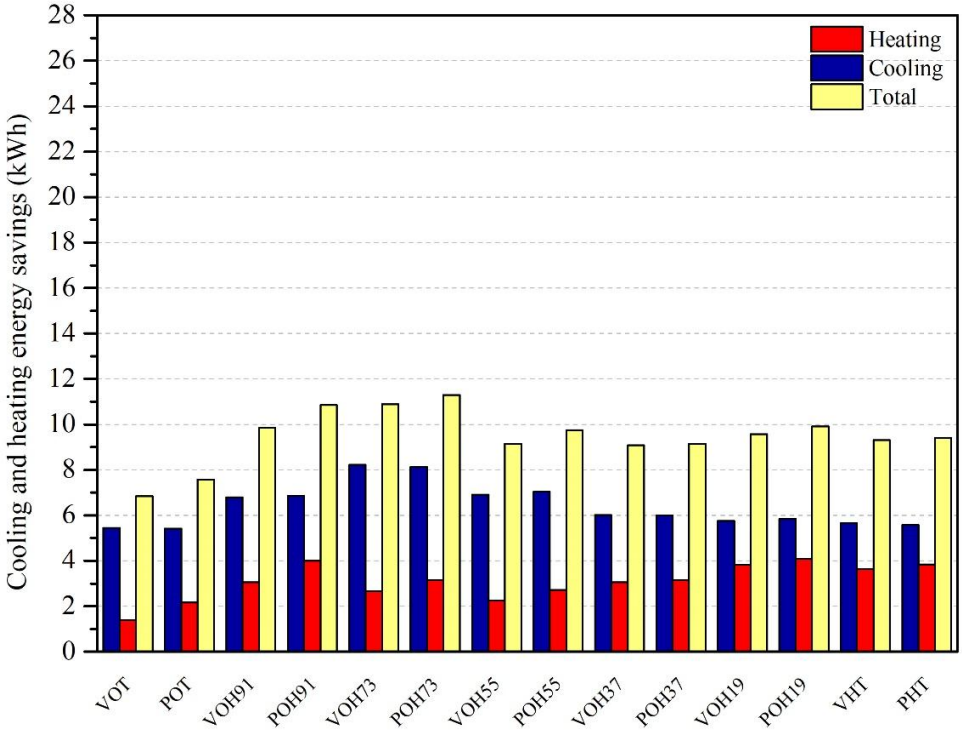

(e) Incheon.

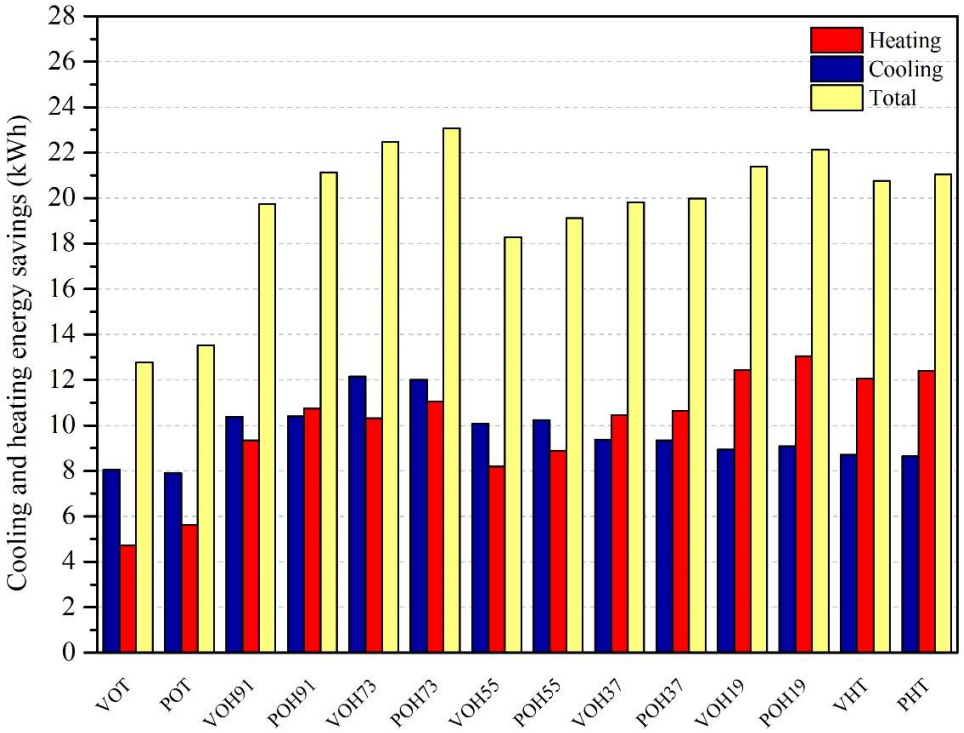

(f) Ulsan.

Figure 13. Cooling and heating energy savings of the building model according to the specimens in (a) Gangneung, (b) Gwangju, (c) Incheon, and (d) Ulsan.

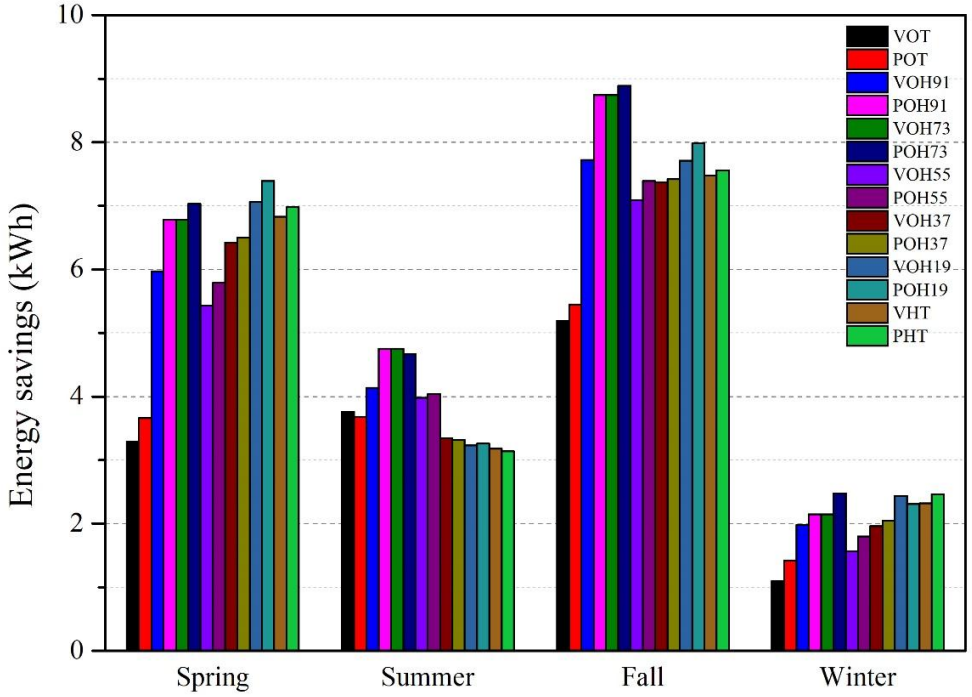

(a) Gangneung.

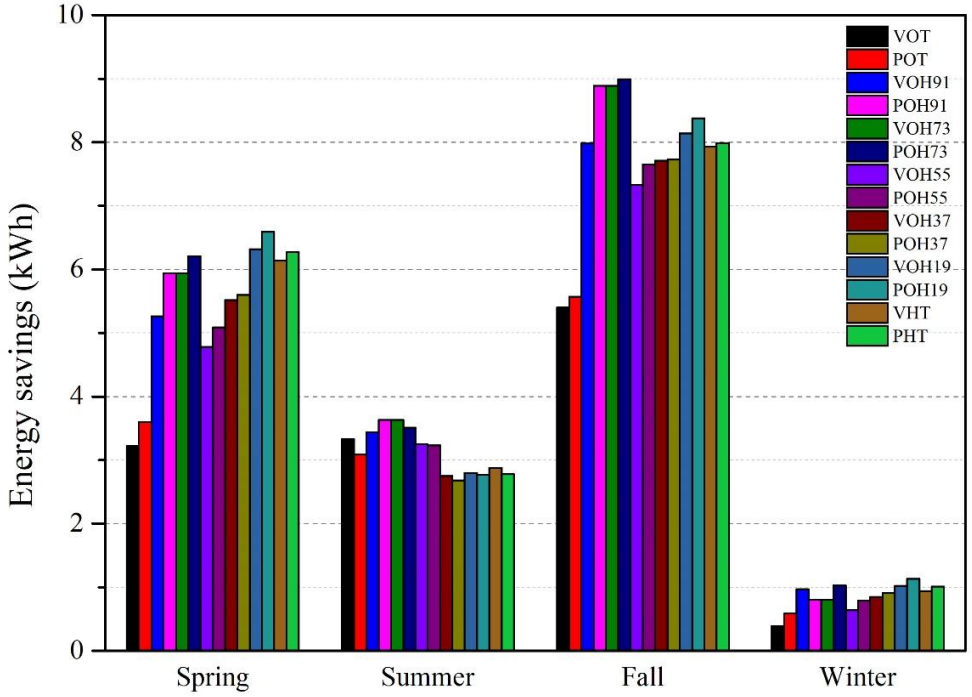

(b) Gwangju.

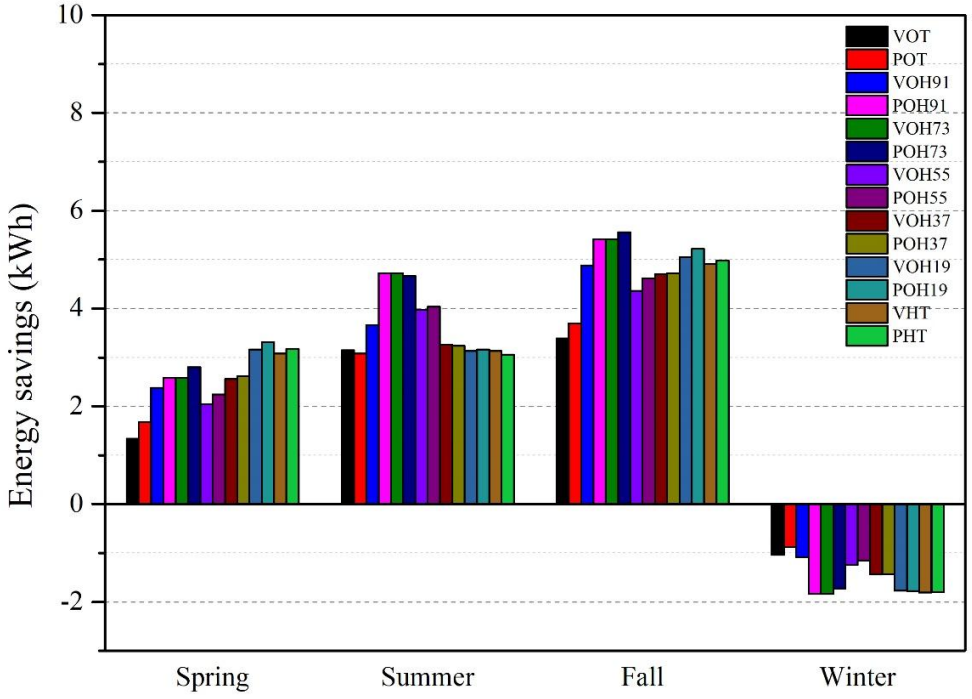

(c) Incheon.

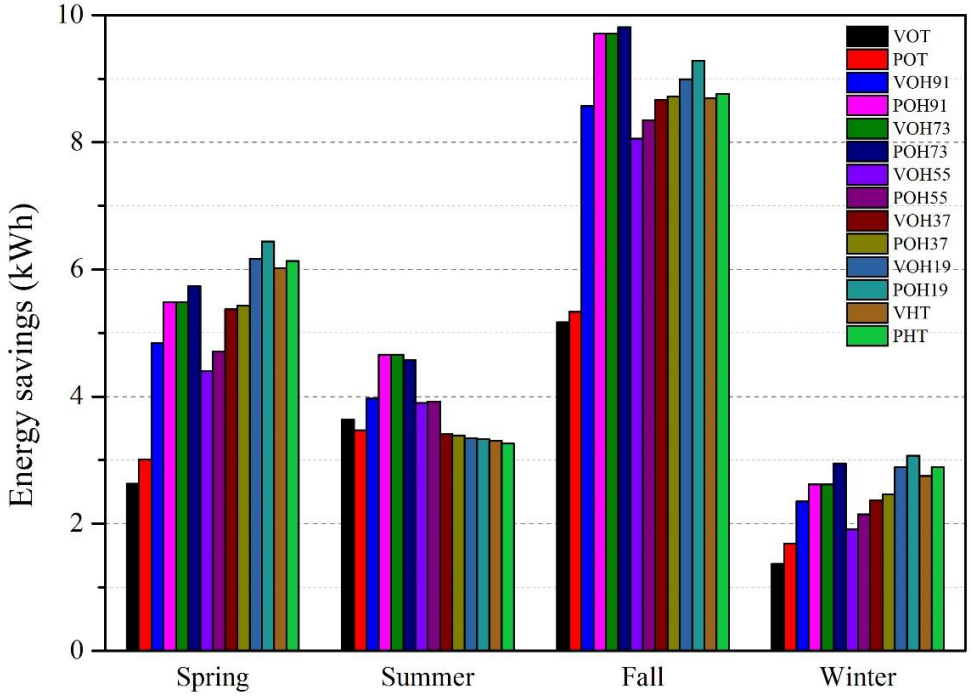

(d) Ulsan.

Figure 14. Energy savings of building model according to the specimens in (a) Gangneung, (b) Gwangju, (c) Incheon, and (d) Ulsan, in four seasons.

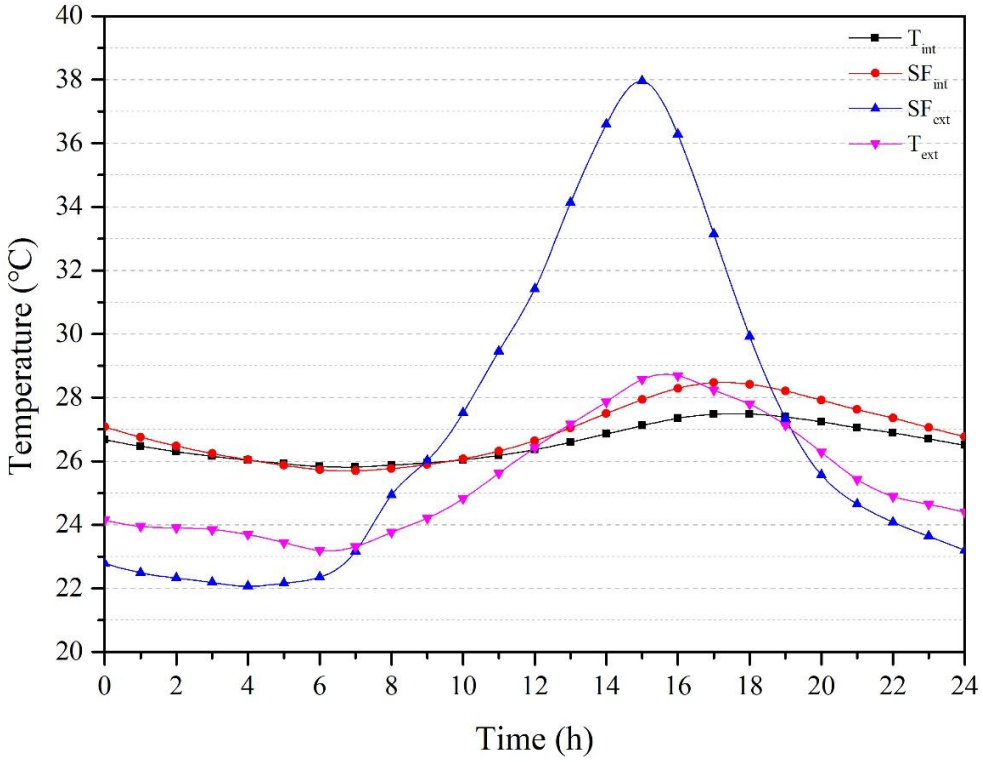

(a) Indoor and outdoor temperature of building model in summer.

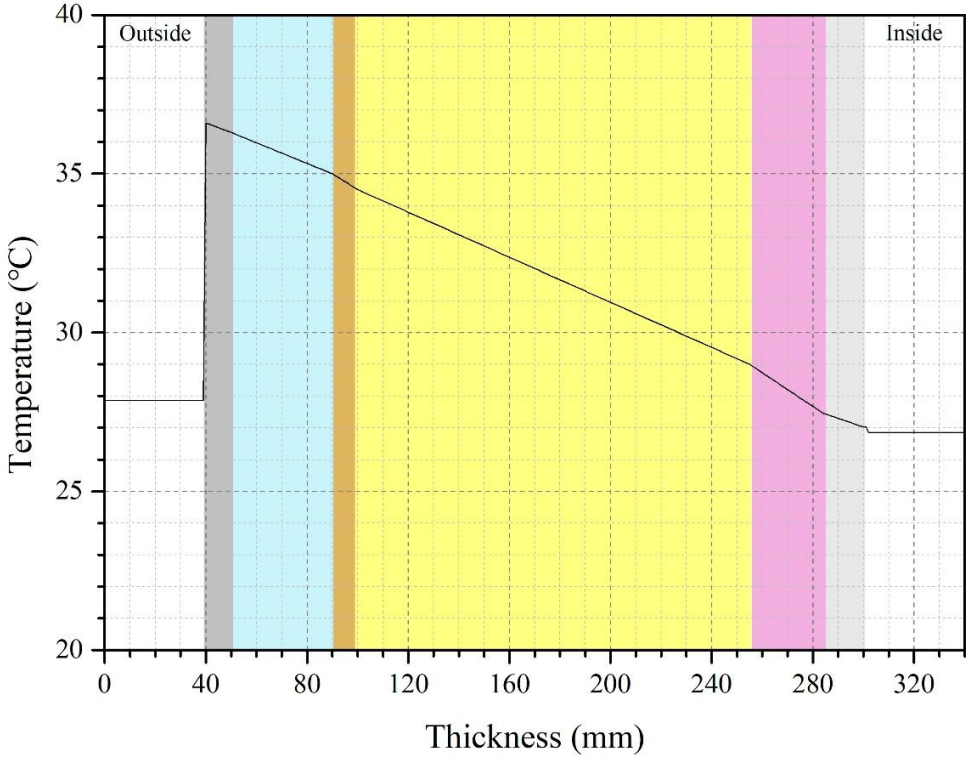

(b) Temperature gradient of building model layers at 14:00 in summer.

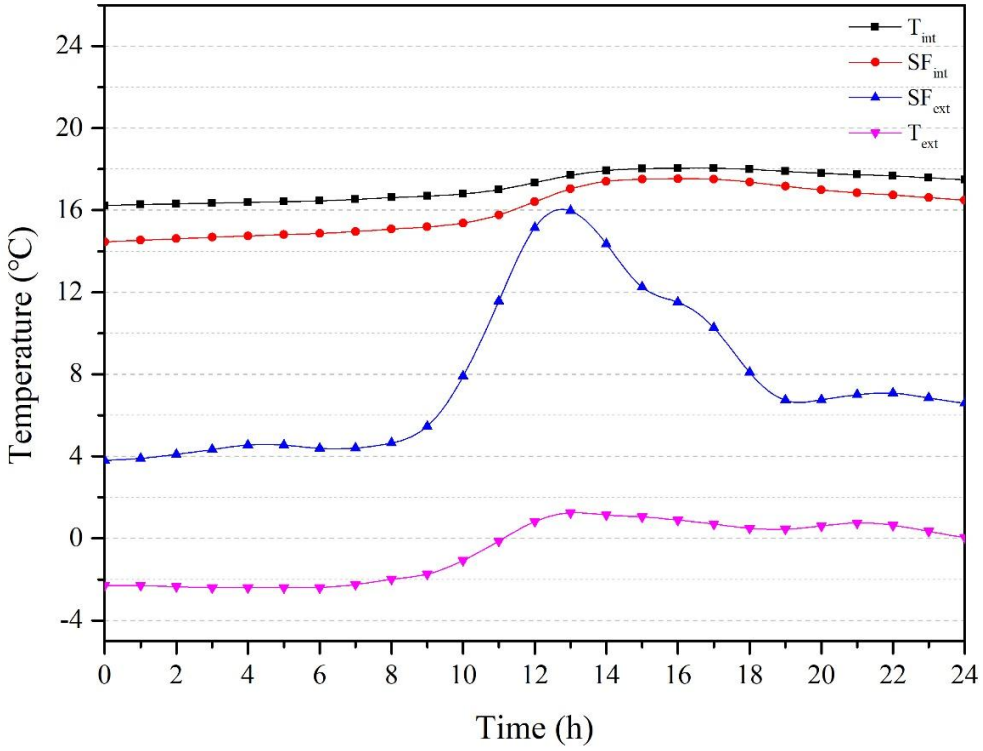

(c) Indoor and outdoor temperature of building model in winter.

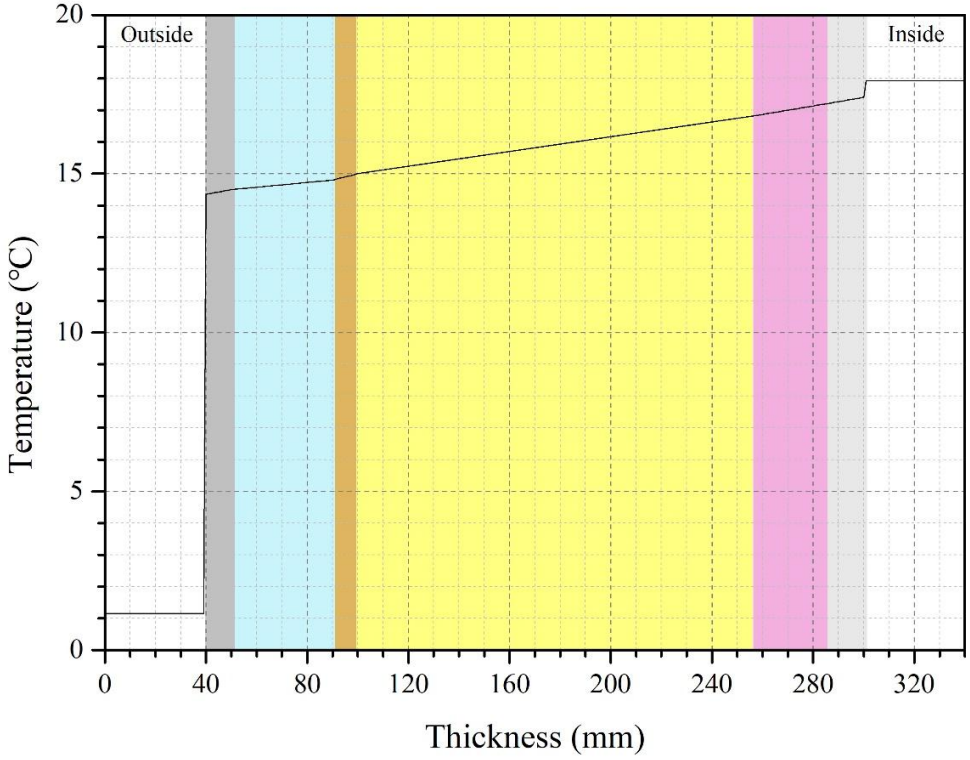

(d) Temperature gradient of building model layers at 14:00 in winter.

Figure 15. Indoor and outdoor temperature of building model in (a) summer and (c) winter; temperature gradient of building model at 14:00 in (b) summer and (d) winter.

Table 1. The physical properties of PCMs.

Specimen	*n*-octadecane	*n*-heptadecane	*n*-hexadecane
Melting temperature (℃)	28.0	22.0	18.0
Latent heat capacity (J/g)	256.5	200.0	257.7
Thermal conductivity (W/mK)	0.26	0.14	0.39
Density (kg/l)	0.77	0.77	0.77

Table 2. Assembly of prepared PCMs for circulation water bath test.

Specimen	*n*-octadecane (g)	*n*-heptadecane (g)	*n*-hexadecane (g)
OT	10		
HT		10	
HX			10
OTHT	5	5	
OTHX	5		5
HTHX		5	5

Table 3. Construction properties of building model.

Construction details	Thickness (m)	U-Value (W/m^2K)
External wall	0.26	0.174
Roof	0.25	0.150
Internal partitions	0.14	1.869
Internal ceiling	0.01	5.333
Ground floor	0.15	0.359

Table 4. Window properties of building model.

Window properties	
Total solar transmission (SHGC)	0.500
Light transmission	0.744
U-Value (W/m^2K)	2.100

Table 5. Climatic conditions of Gangneung, Gwangju, Incheon, and Ulsan.

Cities	Climate values	Jan	Feb	Mar	Apr	May	Jun	Jul	Aug	Sep	Oct	Nov	Dec
Gangneung	Temp. (℃)	0.4	2.2	6.3	12.9	17.6	20.8	24.2	24.6	20.3	15.5	9.2	3.4
	Precip. (mm)	55.1	49.6	68.9	68.7	87.0	120.6	242.8	298.9	243.8	110.4	80.3	38.3
	RH (%)	49.0	52.1	56.6	54.1	61.1	71.4	76.6	78.1	74.3	62.2	53.8	47.8
Gwangju	Temp. (℃)	0.6	2.5	7.0	13.2	18.3	22.4	25.6	26.2	21.9	15.8	9.1	3.1
	Precip. (mm)	37.1	47.9	60.8	80.7	96.6	181.5	308.9	297.8	150.5	46.8	48.8	33.5
	RH (%)	67.7	65.2	62.9	61.9	66.4	72.8	80.0	78.1	74.3	68.4	68.1	68.8
Incheon	Temp. (℃)	-2.1	0.3	5.1	11.3	16.4	20.9	24.0	25.2	21.1	15.0	7.6	0.9
	Precip. (mm)	20.6	20.8	40.5	57.7	100.3	112.0	319.6	285.8	153.5	53.4	51.0	19.3
	RH (%)	61.5	61.8	63.4	64.1	70.3	74.8	82.2	79.1	73.1	67.3	63.9	62.0
Ulsan	Temp. (℃)	2.0	3.9	7.9	13.5	17.9	21.4	25.0	25.9	21.5	16.2	9.9	4.3
	Precip. (mm)	34.3	42.6	65.8	91.1	108.1	176.8	232.3	240.3	168.2	53.5	41.1	23.0
	RH (%)	49.6	51.9	57.6	61.3	66.1	73.3	78.9	77.7	75.7	67.2	59.9	52.4

Table 6. Mixing ratio of OTHT for circulation water bath test.

Specimen	*n*-octadecane (g)	*n*-heptadecane (g)
OH91	9	1
OH73	7	3
OH55	5	5
OH37	3	7
OH19	1	9

Table 7. FTIR spectra of optimized PCMs.

Vibration	Wave number range (cm^{-1})
C-H_3 and C-H_2 asymmetric stretch	2,962±10
C-H_3 symmetric stretch	2,872±10
C-H_2 symmetric stretch	2,855±10
C-H_3 umbrella bending vibration	1,377±10
C-H_2 rocking vibration	720±10

Table 8. Phase change temperature and latent heat capacity of optimized PCMs.

Specimen	Phase change temperature (℃)		Latent heat capacity (J/g)	
	Heating	Cooling	Heating	Cooling
OT	29.81	26.22	247.6	245.8
OH91	26.46	23.42	207.8	194.5
OH73	24.47	22.39	183.2	192.0
OH55	24.33	20.94	171.8	156.5
OH37	22.61	20.15	171.4	169.0
OH19	21.38	19.73	191.1	173.6
HT	21.24	19.52	216.7	213.2

Table 9. Properties of specimens.

Specimen	Density (kg/m^3)	Specific heat capacity (J/gK)	Thermal conductivity (W/mK)
REF	950	1.00	0.200
VOT	937	1.59	0.226
VOH91	920	1.66	0.210
VOH73	922	2.09	0.199
VOH55	941	1.38	0.179
VOH37	954	1.67	0.168
VOH19	920	2.23	0.155
VHT	950	2.00	0.138
POT	959	1.48	0.270
POH91	963	1.54	0.261
POH73	930	1.94	0.228
POH55	990	1.28	0.193
POH37	959	1.56	0.175
POH19	961	2.08	0.164
PHT	962	1.86	0.153

Table 10. Monthly total energy savings of building model in Gangneung.

Energy savings (kWh)	Jan	Feb	Mar	Apr	May	Jun	Jul	Aug	Sep	Oct	Nov	Dec	Annual
VOT	0.21	0.35	0.39	1.42	1.48	1.09	1.40	1.27	2.19	1.82	1.18	0.54	13.33
VOH91	0.42	0.76	0.7	2.62	2.65	1.39	1.45	1.3	2.61	3.05	2.06	0.80	19.81
VOH73	0.40	0.80	0.76	3.02	3.00	1.72	1.65	1.38	3.01	3.46	2.27	0.95	22.42
VOH55	0.31	0.62	0.57	2.39	2.47	1.40	1.38	1.20	2.36	2.92	1.81	0.64	18.07
VOH37	0.37	0.81	0.72	2.91	2.79	1.15	1.15	1.04	2.03	3.06	2.28	0.78	19.09
VOH19	0.43	1.03	0.91	3.31	2.84	1.05	1.13	1.05	1.92	3.05	2.74	0.98	20.44
VHT	0.39	0.99	0.87	3.22	2.74	1.01	1.11	1.09	1.86	2.95	2.67	0.94	19.81
POT	0.30	0.44	0.48	1.59	1.59	1.10	1.41	1.17	2.16	1.88	1.41	0.68	14.21
POH91	0.52	0.93	0.84	2.91	2.83	1.42	1.41	1.22	2.62	3.17	2.40	0.98	21.25
POH73	0.49	0.91	0.86	3.13	3.04	1.71	1.63	1.33	2.97	3.49	2.43	1.08	23.07
POH55	0.37	0.70	0.64	2.56	2.59	1.44	1.40	1.20	2.42	3.01	1.96	0.73	19.02
POH37	0.40	0.84	0.75	2.94	2.81	1.15	1.15	1.02	2.03	3.07	2.32	0.81	19.29
POH19	0.47	1.09	0.96	3.46	2.97	1.07	1.14	1.05	1.95	3.15	2.88	0.75	20.94
PHT	0.43	1.03	0.91	3.29	2.78	1.01	1.10	1.03	1.85	2.97	2.74	1.00	20.14

( ): Negative values.

Table 11. Monthly total energy savings of building model in Gwangju.

Energy savings (kWh)	Jan	Feb	Mar	Apr	May	Jun	Jul	Aug	Sep	Oct	Nov	Dec	Annual
VOT	(0.21)	0.28	0.87	0.88	1.47	1.59	1.13	0.61	1.86	2.15	1.39	0.32	12.34
VOH91	(0.17)	0.50	1.36	1.68	2.22	1.60	1.16	0.68	1.92	3.56	2.5	0.64	17.65
VOH73	(0.35)	0.48	1.53	1.86	2.55	1.75	1.11	0.77	2.02	4.07	2.80	0.67	19.26
VOH55	(0.23)	0.36	1.16	1.52	2.10	1.36	1.07	0.82	1.73	3.33	2.27	0.51	16.00
VOH37	(0.29)	0.44	1.44	1.93	2.15	1.01	0.97	0.77	1.44	3.50	2.77	0.70	16.83
VOH19	(0.35)	0.55	1.77	2.37	2.18	1.00	0.98	0.82	1.46	3.45	3.23	0.82	18.28
VHT	(0.36)	0.52	1.72	2.32	2.10	0.97	1.03	0.88	1.46	3.33	3.14	0.78	17.89
POT	(0.17)	0.37	1.06	0.99	1.55	1.59	1.06	0.44	1.77	2.20	1.60	0.39	12.85
POH91	(0.13)	0.63	1.62	1.88	2.36	1.61	1.09	0.48	1.82	3.70	2.82	0.82	18.70
POH73	(0.30)	0.58	1.67	1.95	2.59	1.74	1.07	0.70	1.94	4.09	2.96	0.75	19.74
POH55	(0.21)	0.42	1.27	1.62	2.20	1.41	1.05	0.77	1.73	3.49	2.43	0.58	16.76
POH37	(0.28)	0.47	1.48	1.95	2.17	1.01	0.92	0.75	1.42	3.50	2.81	0.72	16.92
POH19	(0.34)	0.60	1.86	2.47	2.26	1.02	0.97	0.78	1.45	3.55	3.38	0.87	18.87
PHT	(0.35)	0.55	1.78	2.37	2.12	0.96	1.00	0.82	1.42	3.35	3.22	0.81	18.05

( ): Negative values.

Table 12. Monthly total energy savings of building model in Incheon.

Energy savings (kWh)	Jan	Feb	Mar	Apr	May	Jun	Jul	Aug	Sep	Oct	Nov	Dec	Annual
VOT	(0.45)	(0.28)	0.11	0.77	0.46	1.88	1.13	0.14	1.66	1.01	0.72	(0.31)	6.84
VOH91	(0.47)	(0.29)	0.22	1.23	0.93	2.17	1.24	0.25	1.90	1.97	1.01	(0.32)	9.84
VOH73	(0.74)	(0.47)	0.17	1.38	1.03	2.65	1.58	0.49	2.06	2.24	1.12	(0.63)	10.88
VOH55	(0.49)	(0.35)	0.10	1.07	0.88	2.08	1.35	0.55	1.71	1.85	0.80	(0.40)	9.15
VOH37	(0.58)	(0.41)	0.14	1.35	1.07	1.66	1.07	0.53	1.47	2.18	1.05	(0.45)	9.08
VOH19	(0.72)	(0.50)	0.21	1.72	1.23	1.53	1.05	0.55	1.43	2.34	1.28	(0.55)	9.57
VHT	(0.72)	(0.53)	0.19	1.69	1.20	1.48	1.04	0.61	1.40	2.26	1.25	(0.56)	9.31
POT	(0.43)	(0.17)	0.21	0.95	0.52	1.94	1.11	0.03	1.68	1.11	0.91	(0.28)	7.58
POH91	(0.46)	(0.18)	0.35	1.47	1.01	2.32	1.27	0.11	1.89	2.12	1.25	(0.30)	10.85
POH73	(0.74)	(0.43)	0.26	1.48	1.06	2.68	1.56	0.42	2.03	2.30	1.23	(0.56)	11.29
POH55	(0.47)	(0.33)	0.16	1.16	0.92	2.16	1.37	0.51	1.73	1.95	0.94	(0.35)	9.75
POH37	(0.58)	(0.40)	0.16	1.38	1.08	1.67	1.06	0.51	1.46	2.19	1.07	(0.45)	9.15
POH19	(0.74)	(0.48)	0.24	1.80	1.27	1.58	1.06	0.52	1.45	2.42	1.35	(0.56)	9.91
PHT	(0.73)	(0.51)	0.22	1.74	1.21	1.47	1.03	0.56	1.39	2.29	1.30	(0.56)	9.41

( ): Negative values.

Table 13. Monthly total energy savings of building model in Ulsan.

Energy savings (kWh)	Jan	Feb	Mar	Apr	May	Jun	Jul	Aug	Sep	Oct	Nov	Dec	Annual
VOT	0.10	0.39	0.69	1.10	0.84	1.53	1.39	0.72	1.38	2.12	1.67	0.88	12.81
VOH91	0.15	0.55	1.11	2.28	1.45	1.86	1.43	0.68	1.63	3.48	3.46	1.65	19.73
VOH73	0.10	0.63	1.28	2.49	1.71	2.28	1.52	0.86	1.91	3.93	3.87	1.89	22.47
VOH55	0.05	0.41	0.93	2.08	1.39	1.83	1.26	0.81	1.61	3.26	3.19	1.45	18.27
VOH37	0.02	0.54	1.20	2.67	1.50	1.56	1.08	0.77	1.33	3.41	3.93	1.81	19.82
VOH19	0.06	0.66	1.47	3.23	1.47	1.44	1.08	0.82	1.33	3.33	4.33	2.17	21.39
VHT	0.03	0.62	1.43	3.16	1.43	1.37	1.07	0.87	1.30	3.21	4.18	2.10	20.77
POT	0.16	0.54	0.85	1.25	0.91	1.56	1.38	0.53	1.33	2.16	1.84	0.99	13.50
POH91	0.23	0.75	1.35	2.55	1.53	1.95	1.40	0.55	1.58	3.62	3.79	1.86	21.16
POH73	0.18	0.74	1.41	2.60	1.73	2.29	1.51	0.78	1.86	3.96	3.99	2.03	23.08
POH55	0.09	0.48	1.03	2.22	1.46	1.89	1.26	0.77	1.58	3.39	3.38	1.58	19.13
POH37	0.04	0.57	1.23	2.70	1.50	1.57	1.07	0.75	1.32	3.42	3.98	1.85	20.00
POH19	0.08	0.71	1.56	3.36	1.52	1.47	1.07	0.79	1.33	3.44	4.51	2.28	22.12
PHT	0.06	0.67	1.48	3.22	1.43	1.38	1.06	0.82	1.27	3.23	4.26	2.16	21.04

( ): Negative values.